

1 **Elevational and Oceanic Barriers Shape the Distribution, Dispersal and Diversity of Aotearoa's
2 Kapokapowai (*Uropetala*) Dragonflies**

3
4 Authors: Ethan R. Tolman*^{1,2}, Christopher D. Beatty*^{2,3}, Aaron Goodman*^{2,4}, Priscilla Ramchand*^{2,5},
5 Tara McAllister⁶, Kelly Reyes⁷, Akifa Zahara⁷, Kassandra Taveras⁷, Vincent Wade⁷, John Abbott⁸, Seth
6 Bybee⁹, Robert Guralnick¹¹, Kathleen M. Harding¹², Manpreet K. Kohli^{2,13}, Paul B. Frandsen¹⁰, Jessica
7 Ware^{†2}, Anton Suvorov^{†1}

8 *Equal contributing authors to the manuscript

9 †Senior authors

10 ¹Department of Biological Sciences, Virginia Tech, Blacksburg, Virginia

11 ²Division of Invertebrate Zoology, American Museum of Natural History, New York, New York

12 ³Program for Conservation Genomics, Department of Biology, Stanford University, Stanford, California

13 ⁴The Graduate Center, The City University of New York, New York, New York

14 ⁵Brooklyn College, The City University of New York, Brooklyn, New York

15 ⁶Te Wānanga o Aotearoa, New Zealand

16 ⁷Science Research Mentorship Program, American Museum of Natural History, New York, New York

17 ⁸Alabama Museum of Natural History and Department of Research and Collections, The University of
18 Alabama, Tuscaloosa, Alabama

19 ⁹Department of Biology, Brigham Young University, Provo, Utah

20 ¹⁰Department of Plant and Wildlife Sciences, Brigham Young University, Provo, Utah

21 ¹¹Florida Museum of Natural History, University of Florida, Gainesville, Florida

22 ¹²Redwood City, California, USA

23 ¹³Department of Natural Sciences, Baruch College, New York, New York

24

25 **Acknowledgements**

26 We would like to thank Thomas Beatty and Mahealani Kaloi for their support of this project. We would
27 also like to acknowledge Dr. Milen Marinov for his generosity in providing Odonata specimens, as well
28 as the Department of Entomology at the Smithsonian Institution's National Museum of Natural History,
29 Florida State Collection of Arthropods, and American Museum of Natural History for providing
30 specimens used in this analysis.

31 **Funding**

32 This work was funded by the Graduate Student Research Award from the Society of Systematic
33 Biologists, the Tow Undergraduate and Graduate International Research Stipends from The City
34 University of New York Brooklyn College, the Maxwell/Hanrahan Award from the American Museum of
35 Natural History, and by the National Science Foundation (NSF) Awards [Bybee: 2002432; Ware:
36 2002473; Guralnick: 2002457; Abbott: 2002489: Genealogy of Odonata (GEODE): Dispersal and color
37 as drivers of 300 million years of global dragonfly evolution].

38 **Data availability**

39 Filtered VCF files with and without *P. raptor*, and log and xml files from the BEAST2 runs have been
40 uploaded to figshare (10.6084/m9.figshare.27896910). The Raw reads have been uploaded to the
41 sequencing read archive (bioproject PRJNA1190089).

42 **Conflict of Interests Statement**

43 The authors declare no conflicts of interest.

44

45 **Abstract**

46 Mountains and islands provide an opportunity for studying the biogeography of diversification and
47 population fragmentation. Aotearoa (New Zealand) is an excellent location to investigate both phenomena
48 due to alpine emergence and oceanic separation. While it would be expected that separation across
49 oceanic and elevation gradients are major barriers to gene flow in animals, including aquatic insects, such
50 hypotheses have not been thoroughly tested in these taxa. By integrating population genomic from sub-
51 genomic Anchored-Hybrid Enrichment sequencing, ecological niche modeling, and morphological
52 analyses from scanning-electron microscopy, we show that tectonic uplift and oceanic vicariance are
53 implicated in speciation and population structure in Kapokapowai (*Uropetala*) dragonflies. Although Te
54 Moana o Raukawa (Cook Strait), is likely responsible for some of the genetic structure observed,
55 speciation has not yet occurred in populations separated by the strait. We find that the altitudinal gradient
56 across Kā Tiritiri-o-te-Moana (the Southern Alps) is not impervious but it significantly restricts gene flow
57 between aforementioned species. Our data support the hypothesis of an active colonization of Kā Tiritiri-
58 o-te-Moana by the ancestral population of Kapokapowai, followed by a recolonization of the lowlands.
59 These findings provide key foundations for the study of lineages endemic to Aotearoa.

60 **Keywords**

61 Anisoptera, Epiprocta, biogeography, population genomics, Petaluridae, Islands, Odonata

62 **Introduction**

63 Islands are widely recognized for their unique role in shaping biodiversity (Barreto et al., 2021; Conway
64 & Olsen, 2019; Gleditsch et al., 2022; Wilson, 2009). The Theory of Island Biogeography by MacArthur
65 and Wilson (1963) summarized several of these phenomena, and this theory was later extended to
66 mountaintop habitats (Wyckhuys et al., 2022). The islands of Aotearoa (New Zealand; see table 1 for
67 nomenclature) have often been considered as a natural laboratory to study both island and mountain
68 biogeography (Shepherd et al., 2024; Thomas et al., 2023; Wallis & Buckley, 2024; Waters & Craw,
69 2006). This is due to the opening and closing of Te Moana o Raukawa (Cook Strait) which separates Te
70 Ika-a-Māui and Te Waipounamu (also known as the North and South Islands respectively) and last
71 opened 500,000 years ago (Lewis et al., 1994), and the uplift of Kā Tiritiri-o-te-Moana (the Southern
72 Alps), a relatively young mountain range on Te Waipounamu (South Island; Table 1).

73 Despite its young geologic age, Te Moana o Raukawa has been proposed as a driver of allopatric
74 speciation and population divergence in several taxa including amphipods (Stevens & Hogg, 2004), Weka
75 (terrestrial birds) and their ectoparasites (Trewick et al., 2017), and skink lizards (O'Neill et al., 2008).
76 The tectonic uplift of the Kā Tiritiri-o-te-Moana mountain range likely opened niches and acted as a
77 driver of diversification in flora (Thomas et al., 2023) and fauna (Buckley et al., 2024) of Te
78 Waipounamu. Most lineages of alpine flora arrived in the later Tertiary period, and the environmental
79 upheaval in the Pliocene and Pleistocene drove diversity in these lineages (Thomas et al., 2023). Most
80 alpine invertebrate fauna are relatively young, with ages corresponding to the increased uplift of the Kā
81 Tiritiri-o-te-Moana range 5 million years ago (Ma), and the development of a permanent snow line just
82 over 1 Ma (Buckley et al., 2024). Similar to the flora, it is broadly understood that most invertebrate fauna
83 evolved from lineages already on the island as niches opened with the increased elevation (Buckley et al.,
84 2024), although it has been hypothesized that invertebrates have ridden tectonic uplift to higher altitudes
85 (Heads, 2017).

86 *Kapokapowai as an Important Study System in Island Biogeography*

88 Aquatic insects have been used to better understand the past climate and geology of Aotearoa, and are
89 useful models in the study of evolution and ecology (Córdoba-Aguilar et al., 2022), but they have been
90 relatively underrepresented in biogeographic and broader biodiversity work (Leschen et al., 2023) and
91 knowledge about biogeography remains limited for many taxa. One such group of aquatic
92 macroinvertebrates are the dragonflies first referred to as Kapokapowai (among other names) by Māori
93 (Grant, 2014), and later, named *Uropetala* by scientists from colonial Great Britain and Belgium (Selys
94 1858).

95 Kapokapowai are a particularly promising system for studying the impact of tectonic uplift and
96 oceanic barriers in speciation as a member of the so-called “relict” (Ware et al., 2014) dragonfly lineage
97 Petaluridae, a member of the previously diverse superfamily Petalurida. Petaluridae originated in the mid
98 Jurassic, as sister to the species rich Gomphidae family, but comprising only 11 currently described
99 species (see Tolman et al. (2024) and Cairns et al. (2025) for discussion of the status of one species of the
100 genus *Petalura*) it is among the most species poor lineages of the order Odonata (Tolman et al., 2024).
101 Despite inhabiting fen habitats which should readily promote fossilization, there is only one crown fossil
102 Petaluridae, which is dated to the mid Cretaceous and closely resembles the extant species found at the
103 fossil locality (Tolman et al., 2024). Thus, there is no compelling paleontological evidence that the
104 Petaluridae were previously diverse. Speciation in this family appears to largely be driven by vicariance,
105 as diversification in Petaluridae is strongly correlated with continental drift, and the expansion and
106 contraction of inland seas and land bridges (Ware et al., 2014; Tolman et al., 2024).

107 Kapokapowai likely diverged from the Australian petalurids during continental split between
108 Zealandia and Gondwana, and persisted through the Oligocene drowning of ~18 Ma (Cooper and Cooper
109 1997; Ware et al., 2014; Tolman et al., 2024). Within Kapokapowai there are two currently described
110 species, *Uropetala carovei* (Selys, 1843) which is thought to inhabit lower elevations of both Te Ika-a-
111 Māui and Te Waipounamu (North and South Islands, respectively), and *Uropetala chiltoni* (Tillyard,
112 1921), which inhabits higher elevations of Te Waipounamu (South Island). Kapokapowai is the only
113 lineage within Petaluridae where speciation is thought to have occurred within the past 5 Ma (Tolman et
114 al., 2024), thus the implications of geographical changes on species and population diversity can be
115 studied in finer detail using this species complex than with other lineages of Petaluridae. The study of
116 Kapokapowai can provide important hypotheses for the study of other “relict” lineages on island systems,
117 defined by McCulloch and Waters (2019) to refer to phylogenetically “old lineages” found on
118 geologically “young islands.” Island relicts have been considered to be a high priority for conservation
119 biology (Grandcolas et al. 2014) and for the broader study of extinction and speciation more generally
120 (Grandcolas et al. 2014).

121
122 *Māori Knowledge of Kapokapowai*
123 In systems such as Kapokapowai, Indigenous knowledge is an important source of ecological and
124 evolutionary information (Jessen et al. 2022). According to Māori cosmology, dragonflies and other
125 insects are considered the children of Tāne Māhuta (the god of forests, birds and insects). Dragonflies
126 appear in whakaairo (traditional carvings which often adorn the walls of Māori meeting houses) and
127 waiata (songs) of Māori (Indigenous Peoples of Aotearoa). Stories about dragonflies also feature in
128 pūrakau (legends) belonging to specific iwi (tribes) and hapū (subtribes). All insects, including
129 dragonflies, were created before humans in Māori genealogical histories and are therefore tuakana
130 (roughly translated as an elder family member) and are respected accordingly. Kapokapowai or Kapowai
131 are names commonly-used for the Petaluridae of Aotearoa, which loosely translates to water snatchers,

132 though there are other recorded names including Tītīwaiora, Kihihiwari and Uruururoroa (Grant, 2014).
133 Thus, these historical and cultural accounts provide valuable information about indirect as well as direct
134 spatiotemporal distribution records of Kapokapowai. As this work was conducted with the express
135 permission of the iwi who own the lands of Aotearoa, we refer to these dragonflies by the Māori name,
136 Kapokapowai, in our work here. We also note that the name Kapokapowai was used to describe these
137 dragonflies in the literature by Taylor (1855), italicizing “*Kapokapowai*” as to explicitly refer to a genus,
138 three years prior to the first use of *Uropetala* by Selys (Grant, 2014; Taylor, 1855, 1870), and
139 Kapokapowai has continued to be used to refer to dragonflies in this genus in scientific literature
140 (Durrant, 2024; Fong, 2024; E. R. Tolman et al., 2024). However, we are not making any change to the
141 binary taxonomic nomenclature of this genus here. In referring to Kapokapowai by their Māori name in
142 this work, we designate *U. chiltoni* as Kapokapowai Montaine (KM), and *U. carovei* from either island as
143 Kapokapowai North (KN) and Kapokapowai South (KS; Table 1), representing the three putative species
144 in the Kapokapowai species complex.

145

146 *The Kapokapowai Species Complex*

147 Debate about whether this complex should appropriately be considered to have two species has been
148 ongoing for decades (Andress, 1998; L. S. Wolfe, 1952; Winstanley & Rowe, 1980). According to
149 Tillyard’s original description, KM is characterized by large pale blotches on its labrum, which are not
150 present in KN and KS, and by black femur leg segments, which are brown in KN and KS. However,
151 variation in the splotches of the labrum have been used to suggest that hybrid populations between KM
152 and KS can be found at the north end of Te Waipounamu (Winstanley & Rowe, 1980). Behavioral work
153 suggests that female KM lay all their eggs in one plant, and in repeating this egg laying process females
154 tend to badly damage their wings; such damage has not been seen in KN or KS (W. J. Winstanley, 1981).
155 This behavioral work should be replicated to confirm that this is a species-wide behavior. It has also been
156 suggested that KN and KS may be different species, as KN on Te Ika-a-Māui may have broader superior
157 appendages and larger adult body size than their counterparts on Te Waipounamu (L. S. Wolfe, 1952).
158 Two different karyotypes have been identified for this genus, but it is unclear if this is due to laboratory
159 error (Kuznetsova & Golub, 2020); no other attempts have yet been made to determine the number of
160 species in this genus using molecular data. Based on known morphological variation and behavioral data
161 (L. S. Wolfe, 1952; Winstanley & Rowe, 1980), the dragonflies known as Kapokapowai are hypothesized
162 here to comprise between one and three species, the diversification of which was shaped by both Te
163 Moana o Raukawa (Cook Strait) and Kā Tiritiri-o-te-Moana (Southern Alps).

164 Here, we use population genomics, alongside scanning electron microscopy images of secondary
165 male genitalia, and environmental niche models to determine the number of species and the population
166 dynamics within Kapokapowai and to study how Kā Tiritiri-o-te-Moana and Te Moana o Raukawa may
167 have driven speciation in this genus, and consider how our findings may inform evolution on Aotearoa
168 more generally

169

170 **Materials and Methods**

171 **Population genomics**

172 *Data acquisition*

173 We utilized molecular data from a total of 37 dragonflies, 18 KM, 7 KN, 5 KS, and 7 *Phenes raptor*
174 which were used as an outgroup (Supplemental table 1). We generated a 93 locus, 20kb (on average)
175 nucleotide Anchored-Hybrid Enrichment (AHE) read library (Tolman et al., 2024) for 16 KM, and all

176 other sequenced individuals, following the protocol used by Goodman et al (2023) and Tolman et al.
177 (2024). Briefly, we extracted DNA from one leg of each specimen, which was removed using sterilized
178 forceps, in the case of nymphs and adults. The entire thorax was used to extract DNA from exuvia. We
179 incubated the tissue in proteinase K for one week at 55C, and then followed the manufacturers protocol
180 for the remainder of the DNA extraction using the Zymo DNA Micro-prep kit (Hilden Germany). We
181 sent the DNA extract to RAPID Genomics (Gainesville, Florida) for library preparation and sequencing.
182 Additionally, we incorporated in the current study previously generated 1000 locus (which contained the
183 93 targeted loci for the 35 individuals sequenced here) AHE read libraries for 2 KM individuals, which
184 were used in (Tolman et al., 2024) to estimate phylogenetic relationships of all species of Petaluridae.
185

186 *Population Structure Analysis*

187 We mapped the 37 sequenced AHE read libraries to a previously compiled soft-masked whole genome
188 assembly (NCBI GenBank assembly GCA_036926305.1) of an individual KS (Tolman et al., 2023) with
189 BWA2 (0.7.17-r1188; H. Li & Durbin, 2009) using default parameters, and calculated mapping statistics,
190 average depth and converted the output to a sorted BAM file with samtools v1.16.1 (Danecek et al.,
191 2021). We called variants with bcftools v1.15.1 (Danecek et al., 2021), using the options: bcftools
192 mpileup -a AD,DP,SP -Ou -f reference.fasta Input_bam | bcftools call -
193 f GQ,GP -mO z -o output. We then filtered the resulting VCF file for a minimum quality score of
194 30, and a minimum and maximum depth of 10 and 350 respectively to capture the region targeted with
195 hybrid probes and the adjacent flanking region that is also sequenced and often more variable (Goodman
196 et al., 2023).

197 To visualize population structure we performed a PCA analysis on a covariance matrix generated
198 from the called SNPs with VCFtools v0.1.16 (Purcell et al., 2007) without pruning for linkage-
199 disequilibrium (LD). To test if the outliers in the PCA could be a result of missing data, we identified the
200 missingness of all individuals in the unpruned VCF file which excluded *Phenes*, and compared the
201 missingness of KM with positive and negative PC1 scores. To model the ancestry of each sampled
202 individual, we generated admixture plots for each putative species from admixture models assuming 2-7
203 ancestral populations with ADMIXTURE v1.3.0 (Skotte et al., 2013) and compared model fit using a
204 cross-validation approach. The admixture graph under the best fitting models and the PCA plots were
205 generated in R v2024.04.2+764 using mapmixture v1.1.0 library (Jenkins, 2024). Additionally, we
206 calculated the F_{ST} between and within each of the three putative species both using VCFtools v0.1.16
207 (Purcell et al., 2007). To test for a correlation between genetic and geographic distance among our
208 sampled individuals, we generated pairwise genetic distance matrices between sampled individuals with
209 VCFtools v0.1.16 (Danecek et al., 2021), and then used the Mantel test in the vegan package in R
210 v2024.04.2+764 (Oksanen et al., 2024), with 1,000 permutations to determine the significance of the
211 correlation between geographic and genetic distance.

212 Genetic linkage can bias the recovery of population structure, as can inappropriately pruning sites
213 (Bercovich et al. 2025). To determine the impact of genetic linkage on this dataset, and test the
214 appropriateness of considering SNPs without LD pruning we pruned linked sites with PLINK v1.9.0-b.8
215 (Purcell et al., 2007) using the flags --indep-pairwise 10 5 0 and re-ran the PCA analysis
216 using the resulting VCF file.

217 218 *Species delimitation*

219 To delimit species based on our SNP data, we used the SPEEDEMON v.1.1.1 (Douglas & Bouckaert,
220 2022) pipeline in BEAST2 v2.7.7 (Bouckaert et al., 2014), using all 395 biallelic recovered SNPs after
221 filtering.t.. We used snapper v1.1.4 (Stoltz et al., 2021) to run the SPEEDEMON pipeline on SNPs as
222 opposed to alignments, and BICEPS v1.1.2 (Bouckaert, 2022) to implement a Yule Skyline Collapse
223 Model to test for species delimitations, implemented with a chain length of 10^6 draws. We designated
224 KM as a reference species, with KN and KS as putative species. We used the mean pairwise percent
225 genetic divergence between individuals of KM (~.54), as calculated from the VCF file using the pandas
226 (McKinney, 2010) library for data manipulations and numpy (Harris et al., 2020) for numerical
227 computations, as the prior mean on the theta prior (Douglas & Bouckaert, 2022). We used an alpha of 2.0,
228 and beta of 0.26942 to achieve this mean in the Gamma distribution of the theta prior (see Stoltz et al.,
229 2021 for a full description of these options), and followed the developer's suggestions for all other
230 parameters in the BEAST2 run (Stoltz et al., 2021) . We independently ran the analysis two times to test
231 for model convergence. We computed the posterior mean and upper credible (95%) limit of the Gelman-
232 Rubin-Potential-Scale-Reduction Factor (PSRF) of each parameter, using the coda v0.19.4.1 library
233 (Plummer et al. 2006), in r4.4.1(R Core Team 2021), to test for adequate model convergence.
234 We also calculated the Effective Sample Size (ESS) for both runs in TRACER v1.7.2 (Rambaut et al.,
235 2018) = to test for adequate mixing (at ESS >150) and model convergence (Rambaut et al., 2018).
236

237 *Divergence time estimation*

238 We utilized SNAPPER v1.1.4 (Stoltz et al., 2021) implemented in BEAST2 v2.7.7 (Bouckaert et al.,
239 2014) to determine when the three putative species diverged, and to further explore which populations are
240 most closely related. We used a different SNP set for this analysis, which included seven sampled *Phenes*
241 *raptor* to use as an outgroup. The sequencing and variant call pipeline used to include these samples was
242 identical to the protocol listed earlier. We used PLINK v1.9.0-b.8 (Purcell et al., 2007) with the flags --
243 indep-pairwise 10 5 0.2 to prune linked sites from the VCF containing both *Phenes* and
244 Kapokapowai. We used this pruned input file, with uniform age constraints of 113-135 Ma for the root
245 age and of 0.1-15 Ma for the age of Kapokapowai (as previously identified by Tolman et al. 2024), to
246 generate the snapper input file with a MCMC chain length of 10^7 . SNAPPER can only implement a
247 strict-clock model, a reasonable assumption for recently diverged populations and species, and (Stoltz et
248 al., 2021), and we did not adjust the default tree model employed by SNAPPER. We calculated ESS for
249 both runs in TRACER v1.7.2 (Rambaut et al., 2018) to test for adequate mixing, and computed the
250 posterior mean and upper confidence (95%) limit of the PSRF of each parameter, using the coda v0.19.4.1
251 library (Plummer et al. 2006), in r4.4.1(R Core Team 2021), to test for adequate model convergence.
252

253 *Tests of gene flow*

254 As the resulting tree and species delimitation analyses supported KN and KS as sister, we tested for
255 evidence of introgression between KM and KN and KM and KS with an ABBA-BABA test from Dsuite
256 v0.5 r57, which is optimized to work on lineages with shorter evolutionary time scales. We used the
257 unpruned VCF file which included *Phenes raptor* as input (Malinsky et al., 2021), and used *P. raptor* as
258 an outgroup (E. R. Tolman et al., 2024).
259

260 *Morphological analysis*

261 To identify potential morphological synapomorphies of the putative species of Kapokapowai we
262 evaluated the male secondary genitalia. We specifically looked at the vesica spermalis, or sperm pump.

263 This structure is located on the ventral side of the second abdominal segment in male Odonata, to which
264 sperm is transferred prior to copulation, and may provide informative morphological characters for
265 species determination (Kennedy, 1922; May, 1997; Ware, 2008). The vesica spermalis of Odonata is
266 composed of four segments that are variable between species in their relative size and shape. In
267 Petaluridae, a barb on the second segment near the junction with the third segment and the horns on the
268 lateral side of the third segment have been used to support intrageneric difference (E. Tolman, 2024). We
269 imaged the vesica spermalis (later referred to as penes) from two males from each putative species to try
270 and identify more definitive diagnostic features for species delimitation. We followed the protocol for
271 scanning electron microscopy outlined by Tolman et al. (2024). Briefly, penes were mounted laterally and
272 dorsally on aluminum stubs and coated with gold palladium using a Cressington 108E sputter coater and
273 specimens were then imaged using an S-7400 Hitachi scanning electron microscope.

274

275 ***Environmental niche modeling***

276 *Occurrence Records*

277 We acquired occurrence records of adult KN, KS, and KM from the Global Biodiversity Information
278 Facility (GBIF)(available in Supplemental data). We selected occurrences from GBIF possessing
279 preserved museum samples and research grade observations, which include verified latitude and longitude
280 coordinates, a photograph of the sighting, observation date, and at least $\frac{2}{3}$ agreement on species
281 identification by the community. We filtered occurrences by removing sightings from erroneous localities
282 (middle of the ocean, locations of large museums). We divided occurrences for KN and KS between Te
283 Ika-a-Māui and Te Waipounamu (North and South Islands) to be used as individual models
284 (Supplemental Table 3).

285

286 *Environmental Data*

287 We acquired averaged sets of environmental predictor variables for modeling consisting of purely
288 bioclimatic variables. All analyses were conducted using the statistical programming language R v. 4.1.2.
289 We acquired environmental rasters at 2.5 arc-second resolution (~5km at the equator) from the CHELSA
290 climate database v2.1 (Karger et al., 2017, 2023) . We downloaded the ‘Anthropocene’ bioclimatic
291 dataset (1979 – 2013) consisting of 19 bioclimatic variables which follow Worldclim v2 (Fick &
292 Hijmans, 2017). We omitted bioclimatic variables 8 and 9 after visual inspection of interpolation
293 discontinuities (Booth, 2022). Although such spatial artifacts were minor within our initial study extent,
294 we observed major breaks of climate smoothing when we extrapolated our model to a larger spatial extent
295 within the last glacial maximum and interglacial periods.

296

297 *Model Construction*

298 We spatially thinned occurrences to the resolution of our environmental variables to reduce the effects of
299 sampling bias and artificial clustering (Veloz, 2009). We thinned occurrences by 5km to match the spatial
300 resolution of our environmental data. We chose study extents for occurrences of KN and KS found in Te
301 Ika-a-Māui and Te Waipounamu, defined as polygons around all localities between both islands
302 respectively; we chose the same study extent for occurrences of KM found in Te Ika-a-Māui. We chose
303 these study extents to include potential suitable habitat, while excluding large areas outside the species’
304 dispersal limitations (Peterson & Lieberman, 2012). Within this extent, we randomly sampled 50,000
305 background points for modeling and extracted their environmental values. We used these values to
306 calculate correlations between variables using the ‘vifcor’ and ‘vifstep’ functions in the usdm package

307 (Naimi, 2023) and filtered out variables with correlation coefficients higher than 0.7 and a Variance
308 Inflation Factor (VIF) threshold of 10, both standard cutoffs in such analyses (Goodman et al., 2024).

309 To model the distribution of putative Kapokapowai species, we used the presence-background
310 algorithm MaxEnt v3.4.4 (Phillips et al., 2017), using the R Package ENMeval 2.0.0 (Kass et al., 2021)
311 for model building, parameterization, evaluation with different complexity settings, and reporting of
312 results. We partitioned our data using the ‘checkerboard2’ strategy. To prevent our model from
313 extrapolating beyond the bounds of training data, we clamped our models by omitting ranges of
314 environmental data which fall outside of the training data. All final models were fitted to the full dataset.
315 We tuned model complexity to find optimal settings using different feature classes, including linear (L),
316 quadratic (Q), and hinge (H) as well as regularization multipliers 1 through 5 (higher numbers penalize
317 complexity more) (Radosavljevic & Anderson, 2014; Warren & Seifert, 2011).

318 We assessed our model using averages of threshold-dependent (omission rate) and
319 threshold-independent (Area Under the Receiver Operating Characteristic or AUC) discrimination
320 performance metrics calculated on withheld validation data (Warren & Seifert, 2011). The 10th-percentile
321 omission rate sets a threshold as the lowest suitability value for occurrences after removing the lowest
322 10% suitability values (Kass et al., 2021; Radosavljevic & Anderson, 2014). Validation AUC is a
323 measure of discrimination accuracy that can be used to make relative comparisons between ENMs with
324 different settings fit on the same data (Lobo et al., 2008; Radosavljevic & Anderson, 2014). Finally, we
325 checked the results against the Akaike Information Criterion with correction for small sample sizes
326 (AICc; calculated on the full dataset) (Warren & Seifert, 2011). To investigate model behavior, we
327 examined marginal response to suitability. Marginal response curves show the modeled relationship of
328 each variable individually with the occurrence data when all other variables are held constant (Phillips et
329 al., 2017).

330 We made habitat suitability predictions for KM, and KN and KS from both islands using our
331 ‘Anthropocene’ environmental predictor variables. We projected our modern-day models to a new study
332 extent to encapsulate the potential habitat of Kapokapowai within the historic past, defined as a polygon
333 around both Islands of Aotearoa. We generated thresholdless predictions by converting raw predictions to
334 a scale of 0-1 to approximate probability of occurrence using the ‘cloglog’ transformation (Phillips et al.
335 2017). We also generated a threshold prediction, calculated from the 10-percentile omission rate from our
336 model evaluation. To estimate habitat suitability of Kapokapowai within the geologic past, we generated
337 predictions using environmental predictor variables from the PaleoClim dataset (Brown et al., 2018). We
338 generated predictions within three distinct time periods: Mid-Holocene (8.3 – 4.2ka), Last Glacial
339 Maximum (21ka), and the Last Interglacial (130ka).

340

341 *Ordination Analysis*

342 To determine niche differentiation between putative species, we compared niche overlap in occurrences
343 of KN and KS from Te Ika-a-Māui and Te Waipounamu using an ordination framework by first reducing
344 dimensionality within the datasets via a Principal Component analysis (PCA). Using the ‘espace_pca’
345 function in the *Wallace* v2.0.5 and *ade4* package v1.7 in R (Dray & Dufour, 2007; Kass et al., 2018)), we
346 generated a Principal Components Analysis (PCA) using environmental variables from Kapokapowai
347 occurrences and plotted with correlation loadings to infer the degree of influence particular environmental
348 variables possess in the distribution of the 50,000 background points within niche space; we chose
349 bioclimatic variables which were uncorrelated and shared among both Kapokapowai MaxEnt models.
350 Using the ‘espace_occDens’ function in the package *ecospat* v3.2 (Di Cola et al., 2017, p. 2) an

351 occurrence density grid was estimated for both the environmental values at each occurrence point and
352 background extent points using a kernel density estimation approach. Niche overlap between occurrence
353 density grids of environmental values at each occurrence point and background points were compared
354 using Schoener's D (Schoener, 1968) 'espace_nicheOv' function. Finally, using the
355 'ecospat.plot.overlap.test' function, we conducted a niche similarity test in which Kapokapowai niches
356 from both islands are randomly shifted in the background extent and permuted 1000 times, and the niche
357 overlap between the two are recalculated. A p-value <0.05 indicates that the niches from both time
358 periods are significantly similar with each other.
359

360 *Ancestral State Reconstruction of Elevation Ranges in Petaluridae*
361 Having considered the niche space and population structure of low and high elevation Kapokapowai, then
362 determined whether inhabiting mountains (KM) or lowlands (KN and KS) is the ancestral state for
363 Kapokapowai—an important consideration in how these dragonflies are impacted by geography—by
364 conducting an ancestral state reconstruction of the maximum elevation range for all of Petaluridae. We
365 downloaded all occurrences of Petaluridae from the Global Biodiversity Information Facility (GBIF;
366 GBIF.org, 2025) and determined the elevation of each occurrence point using the elevatr v0.99.0 R
367 package (Hollister et al. 2023). We determined the 90th percentile of elevation for each species of
368 Petaluridae to minimize the impact of outlier observations, and classified the species as occupying high
369 (>900 M), medium (400-900 M) or low (<400 M) elevations based upon this statistic. To model ancestral
370 states we fit three variants of the Markov k-state model: Equal-Rates (ER), a single transition rate
371 between all pairs of states, Symmetric-Rates (SR), distinct forward and backwards rates that are equal in
372 reciprocal pairs; All-Rates-Differed (ARD), allowing each transition a unique rate. We fit each model
373 with phytools v2.4-4 (Revell 2012) with estimated stationary frequencies. We also fit a custom model
374 with equal rates between low and medium elevation, medium and high elevation, and a different rate
375 between low and high elevation. We then compared model fit for the four models using AIC and used
376 model averaging from ANCR to integrate node-state estimates across models according to their AIC
377 rates. We used the dated species tree for Petaluridae (including the two currently described species of
378 Kapokapowai) from Tolman et al. (2024) and added *Petalura pulcherrima* as sister to *P. ingentissima* at
379 14 Ma (within the confidence interval identified by Ware et al. (2014)). We tested the model with and
380 without the fossil *Argentinopetala archangelskyi* which has been identified as sister to *P. raptor* (Tolman
381 et al., 2024). To determine the elevation of this fossil at ~115 Ma we converted the modern coordinates
382 into the paleo-coordinates at 115 Ma using the palaeorate function in palaeoverse v1.4 (Jones et al. 2023)
383 with grid rotation under the MERDITH2021 plate model. We used raster v3.6.31 (Hijmans, 2025) to load
384 the 1° resolution Early Cretaceous Digital Elevation Model (DEM; Scotese and Wright 2018) and extract
385 the paleo-elevation at the rotated point. As all states were equally probable at each internal node with and
386 without *A. archangelskyi*, we reconduted searches with the averaged model using stochastic character
387 mapping. To infer the frequency of changes between character states, we simulated 1000 discrete
388 character histories under the selected averaged model, with empirical root-state frequencies set using the
389 fitzjohn option in phytools v2.4-4 (Revell 2012). All aforementioned ancestral state reconstruction
390 analyses were conducted in R v4.4.1 (R Core Team 2021).

391

392 **Results**

393 *Population genomics*

394 *Population Structure Analysis*

395 Mean sequencing depth varied from 0.02x to 0.19x, and missingness (calculated from the LD pruned
396 VCF file) ranged from 0.01 to 0.27 (Supplemental Table 1). After filtering for mapping quality ($> q30$)
397 and depth (10-350), we retained 365 SNPs for the initial population structure analysis. The weighted F_{ST}
398 values were estimated at 0.23 between KM and KS, 0.29 between KM and KN and 0.11 between KN and
399 KS (Table 2). We then separated the data into subsets as follows by their distributions along PC1 (Fig
400 1A): KM (all individuals), KM (negative PC axes), KN (Te Ika-a-Māui) and KS (Te Waipounamu). The
401 F_{ST} values differed when only a subset of KM was used (Supplemental Table 3). There was no evidence
402 that geographic separation was correlated with pairwise genetic distance within Kapokapowai (Pearson's
403 correlation coefficient $r = 0.02462$, p-value = 0.322).

404 The centroid of KM was distal from the centroids of KN and KS across PC1, while the centroid
405 of KN and KS differed along PC2 (Fig. 1A). Despite the differing centroids across PC1 and PC2, there
406 was overlap in the space occupied between all three putative species (Fig. 1A). The missingness of KM
407 individuals with a positive PC1 ranged from 0.02 to 0.17, while the missingness of KM individuals with a
408 negative PC1 value ranged from 0.07 to 0.16 (Supplemental Table 3). 118 SNPs were retained after LD
409 pruning the VCF, although the resulting population structure visualized through PCA (Supplemental Fig.
410 1) largely reflected the structure generated from pruned SNPs (Fig. 1A), with a slightly reduced distance
411 between KN and KS.

412 Because of the low cross validation-error indicating comparable fit to other tested models
413 (Supplemental table 5), and the three clusters identified in our PCA analysis, we provide the three
414 ancestral populations model in our main figure and discussion (Fig. 1B), but also provide assumptions of
415 $K = 2$, and $K = 4$ (Supplemental fig. 2). Ancestral population 1 was only present in KM, while ancestral
416 populations 2 and 3 were present in all three putative species (Fig. 1B).

417 *Species delimitation analysis*

418 All parameters in the SPEEDEMON analysis showed adequate mixing (ESS > 400), and model
419 convergence (PSRF = 1.0 with 95% CI < 1.01 for all parameters). The species were recovered as currently
420 described, specifically KM as *U. chiltoni* and KN and KS as *U. carovei*, with very high (99%) posterior
421 support.

422 *Divergence time estimation*

423 Including the outgroup *Phenes raptor* we recovered 727 SNPs and retained 204 of these SNPs after LD
424 pruning. The SPEEDEMON runs showed adequate mixing (ESS > 600 for posterior, likelihood, prior,
425 lambda and tree height; ESS > 150 for clock rate) and strong evidence of convergence (PSRF = 1.0 with
426 95% CI < 1.06 for all parameters). In the dated tree Kapokapowai and *Phenes* shared a Most Recent
427 Common Ancestor (MRCA) between 113.0 and 133.7 Ma, KM shared a MRCA with KN and KS
428 between 2.6 and 15.0 Ma, while KN and KS diverged between 0.1 and 3.2 Ma (Fig. 1E; Supplemental
429 Fig. 2).

430 *Tests of gene flow*

431 The ABBA-BABA test, implemented in D-suite using all 727 SNPs identified evidence of gene flow
432 between KM and KS ($p < .01$; Table 2)). It is important to note that this test cannot determine the
433 directionality of gene flow.

434

435

439 Figure 1: Population Genomics of Kapokapowai

440

441 Fig. 1: (A) PCA of Kapokapowai from SNPs, colored by putative species: Kapokapowai Montane (Blue),
442 KN (Green) and KS (Teal). Each dot represents one individual with the distance from each point to the
443 centroid of each putative species shown with a line. (B) Admixture analysis of Kapokapowai assuming
444 three ancestral populations, with the ancestral populations 1-3 colored as blue, green, and teal respectively
445 per each sampled individual (x-axis). Pie charts are mapped according to their proximate locality, and
446 represent the proportion of each ancestral population in the gene pool of each locality. Ancestral
447 population 1 is only found in KM. (C) Adult Female Kapokapowai North from Te Ika-a-Māui. (D)
448 Nymphs of Kapokapowai Montane. (E) Dated tree displaying the divergence between the three putative
449 species and the outgroup *Phenes raptor*. Notable geographic events in Aotearoa are annotated on the tree,
450 including the Oligocene drowning when Aotearoa was reduced to 18% of its current size (Cooper and
451 Cooper 1997), the reemergence of taxa following the drowning, the uplift of Kā Tiritiri o te Moana, and
452 the Pleistocene land bridge events between Te Ika-a-Māui and Te Waipounamu.

453

454

455 *Morphological analysis*

456

457 *Figure 2: Male Secondary Genitalia of the Three Hypothesized Kapokapowai Species*

458 *Scanning electron microscopy.* Images of male penes from six sampled Kapokapowai (two from each
459 putative species). Divergent features include (1) curves at the end of the horns only found in
460 Kapokapowai Montane, (2) the barb near the joint of the second and third segments, and (3) a knob found
461 near the barb from one individual from Kapokapowai North.

462

463 The “horns” of KM (see figure 2, feature 1) are downcurved at the tips in a way not observed in any of
464 the three KN or KS individuals (Fig. 3). The angle and curvature of the barb (figure 2, feature 2), and the
465 presence of a “knob” near it (figure 2, feature 3) differs between individuals, but does not appear to be
466 fixed between any populations. One individual of KN had a knob near the barb.

467

468 *Ecological Niche Modeling*

469 Optimal model settings varied considerably for Kapokapowai based on 10-percentile omission rate and
470 mean validation AUC metrics. Based on the results of the collinearity analysis, we used the following six
471 predictor variables to build all models: Isothermality (bio03), temperature seasonality (bio04), maximum
472 temperature of the warmest month (bio05), precipitation seasonality (bio15), precipitation of the warmest
473 quarter (bio18), and precipitation of the coldest quarter (bio19). Models varied in complexity with
474 expressing either hinge-loss, or linear-quadratic feature classes with regularization multipliers of 3-4
475 (higher complexity penalty). Mean validation AUC was adequate for KS and KM (0.75 and 0.86
476 respectively), while 10% omission rate was low relative to its expected value of 0.1 (0.11 and 0.09
477 respectively) (Supplemental Table 2). Furthermore, optimal models for KS and KM possessed low
478 amounts of non-zero lambdas (coefficients) and AICc values suggesting low amounts of model
479 overinflation (Supplemental Table 2). Optimal models for KN performed poorly, possessing an
480 unacceptably low AUC value (0.44) and high 10% omission rate (0.16) (Supplemental Table 2).

481 Optimal models retained 4 – 6 predictor variables after regularization, and relied mainly on
482 contributions from Isothermality (bio03), temperature seasonality (bio04), maximum temperature of the

483 warmest month (bio05), and precipitation of the wettest and driest quarters (bio18 and bio19 respectively)
484 (See Supplemental Fig. 3). Response curves of climate variables revealed differing relationships with
485 suitability among Kapokapowai models (Supplemental Fig. 1). Response curves for KN expressed jagged
486 optimal ranges, with habitat suitability not following a smooth or continuous gradient. Temperature
487 Seasonality (bio03) and precipitation of the coldest quarter expressed positive linear/hinge relationships
488 with suitability among all three Kapokapowai models, while precipitation of the wettest quarter (bio18)
489 expressed negative linear/hinge relationships with suitability for KN and KS; precipitation of the wettest
490 quarter possessed no relationship in KM. Isothermality (bio03), and maximum temperature of the
491 warmest month (bio05) expressed opposite relationships with suitability within Kapokapowai.
492 Isothermality (bio03) expressed positive linear or linear/quadratic relationships with suitability within
493 KM and KN, but a negative linear relationship with KS. Maximum temperature of the warmest month
494 (bio05) expressed negative linear or quadratic/linear relationships with suitability within KM and KS but
495 a positive linear relationship within Kapokaowai South (Supplemental Fig. 1).

496 Predictions using our ‘Anthropocene’ environmental variables for KS within Te Waipounamu
497 revealed areas of high suitability along the coast (Westland, Nelson and Marlborough provinces) (Fig
498 3D). Suitability was highest for KM across the Southern Alps (interior Nelson and Marlborough
499 provinces) (Fig. 3A). Predictions for Kapokaowai North within Te Ika-a-Māui revealed areas of high
500 suitability within the interior (Wellington and Hawke’s Bay, along the Tararua, Ruahine, and
501 Kaimanawa Mountain Ranges), as well as the Northern portion of the island within Auckland (Fig 3G).
502 Threshold predictions reflect our ‘cloglog’ predictions (See Supplemental Fig. 3).

503 Predictions generated from our paleoclimate variables demonstrated variability in suitability over
504 time for Kapokapowai compared to our modern-day ‘Anthropocene’ variables. For KM, suitability
505 expands within the mid-Holocene (8.3 – 4.2ka), encompassing most of Te Waipounamu except for the
506 coastal margins (Fig 3H.). Projection to the Te Ika-a-Māui within the mid-Holocene indicates suitable
507 habitat within the island’s center (Te Ika-a-Māui Volcanic Plateau, Tararua Range, and Raukumara
508 Range) (Fig 3H.). Within the LGM, suitability contracts within Te Waipounamu, with suitable habitat
509 only being located within a small portion of the Kā Tiritiri-o-te-Moana (Southern Alps) and Kaikōura
510 Mountain Ranges (Fig 3I.). Within Te Ika-a-Māui, suitability expands, encompassing most of the western
511 and southern mountain ranges. Although a land bridge connected both Islands during the LGM (Te
512 Moana o Raukawa), suitability was low (Fig 3I.) while our threshold predictions suggest suitable habitat
513 across the strait (See Supplemental Fig. 4).

514 For KS within Te Waipounamu, suitability contracts within the mid-Holocene, being restricted to
515 a small portion of the coast (northern Westland) (Fig 3E.). When projected to Te Ika-a-Māui, suitability is
516 high within the Northern Cape and southwestern cape (Taranaki Province), and Auckland (Fig 3E.).
517 Within the LGM, suitability expands encompassing the northern coastal regions of Te Waipounamu
518 (Westland and Nelson), as well as the Northern Cape, Taranaki Province, and Auckland within Te Ika-a-
519 Māui (Fig 3F.). Suitability across the Te Moana o Raukawa is intermediate, with a few pockets of high
520 suitability (Fig 3F.) while our threshold predictions suggest suitable habitat across the strait (See
521 Supplemental Fig. 4).

522 For KN within Te Ika-a-Māui, suitability contracts within the mid-Holocene, with only a few
523 pockets of high suitability within the southern coasts (Tararua Ranges), and Auckland (Fig. 3B.). When
524 projected to Te Waipounamu, suitability is highest along the coastal ranges of southern Westland and
525 Otago. Within the LGM, suitability expands to include most of the southern Mountain Ranges within Te
526 Ika-a-Māui, as well as Kaimanawa Mountain Ranges within the middle of the Island (Fig 3C). Within Te

527 Waipounamu, suitability slightly expands southward into the coastal ranges of Otago (Fig 3D). Suitability
528 within the Te Moana o Raukawa remains intermediate with a small pocket of high suitability off the coast
529 of Taranaki (Fig 3D.) while our threshold predictions suggest suitable habitat across the strait (See
530 Supplemental Fig. 4).

531

532 *Ordination Analysis*

533 Environmental variables for KN and KS within Te Ika-a-Māui and Te Waipounamu expressed an
534 intermediate degree of overlap in ordination analysis, but were statistically more similar than random
535 (Fig. 4). Within our PCA analysis, the first principal component explained ~34% of the variance with
536 PC2 explaining ~32%. Isothermality (bio03), temperature seasonality (bio04), and precipitation of the
537 coldest quarter (bio19) loaded strongly on PC1, while precipitation of the warmest and coldest quarters
538 (bio18 and bio19) loaded strongly on PC2 (Table 4). Environmental niche overlap for Kapokapowai was
539 intermediate between Te Ika-a-Māui and Te Waipounamu (Schoener's $D = 0.24$), with niche similarity
540 tests showing observed overlaps being higher than 95% of simulated overlaps ($P = 0.01$), supporting
541 niche similarity between both islands (Fig. 4).

542

543 *Figure 3: Niche Models of Kapokapowai Populations.* MaxEnt predictions for Kapokapowai projected to
544 the modern day using our 'Anthropocene variables', mid-Holocene (Northgrippian: 4.2 – 8.326ka)
545 generated from the PaleoClim dataset (Brown et al. 2018), and Last Glacial Maximum (LGM)(21ka) and
546 Last Interglacial (LIG)(130ka) generated from the CHELSA database (Karger et al. 2017). Predictions
547 were derived from the optimal model using the criterion of mean valuation AUC (AUC_{val}) values being
548 the highest, and 10% omission rate being the lowest. Predictions were transformed using the 'cloglog'
549 function in Maxent v3.4.4 (Phillips et al., 2017), in which raw values are converted to a range of 0 - 1 to
550 approximate a probability of occurrence. Brighter colors (yellow, green, blue) indicate areas of higher
551 suitability (higher probability of occurrence), while darker colors (violet) indicate areas of lower
552 suitability (lower probability of occurrence).

553

554 *Figure 4: Niche Overlap of Kapokapowai North and Kapokapowai South.* Ordination plot (PCA), niche
555 overlap, correlation circle, and niche similarity tests showing niche differences between Kapokapowai
556 North and South from Te Ika-a-Māui (North) and Te Waipounamu (South). Ordination plot represents
557 principal component points of occurrence and background environmental values using type 2 scaling
558 (Mahalanobis distance). PCA points for Te Waipounamu are in blue, while Te Ika-a-Māui is red. Solid
559 contour lines in the niche overlap illustrate full range (100%) of climate space ('fundamental niche')
560 while dashed lines indicate 50% confidence intervals. Contour lines of Te Waipounamu are in orange,
561 and Te Ika-a-Māui is blue. Shading shows the density of species occurrences per grid cell of kernel
562 density analysis ('realized niche'), and violet pixels show niche stability (climate conditions occupied in
563 both time periods). Orange shading indicates climate conditions only occupied by Te Waipounamu, while
564 blue indicates climate conditions only occupied by Te Ika-a-Māui. Correlation circle indicates climactic
565 variable loadings on the PCA space. Length and direction of arrows indicates influence and distribution of
566 variables within PCA space. Bioclimatic variables which follow Worldclim v2 (Fick and Hijmans 2017).
567 Histograms represent observed (red bar) and randomly simulated overlaps of niche similarity. The
568 observed overlap is higher than 95% ($p < 0.05$) for both analyses supporting the niche similarity across
569 both islands.

570

571 *Ancestral State Reconstruction*

572 Figure 5: *Ancestral State Reconstruction of the Maximum Elevation inhabited by Petaluridae*. Maximum
573 likelihood (ML) reconstructions and stochastic character mapping (SM) are shown both with (ML A, SM
574 B) and without (ML C, SM D) the fossil taxa *Argentinopetala archangelskyi*, which is considered to be
575 sister to *P. raptor* based upon wing characteristics (Tolman et al., 2024). In all models, all three ancestral
576 states (high, medium, and low maximum elevation) are equally likely as the ancestral state at each node,
577 including at the root.

578

579 The ER model was strongly supported by AIC (Supplemental Table 6) both with and without *A.*
580 *archangelskyi*, indicating gains and losses of different elevation habitats are equally probable across the
581 tree. All nodes were equivalent with near equal support for each elevational maximum, including the
582 ancestral state of Petaluridae, in both maximum likelihood models and using stochastic character
583 mapping, both with and without *A. archangelskyi* (Fig. 5). Across 1000 stochastic maps under the
584 averaged model with *A. archangelskyi* included in the tree, we inferred on average 235 instances of
585 medium to high elevation and high to medium elevation with transition and 236 medium to low and low
586 to medium transitions, meaning each of these transitions are expected to occur once every 2.9 million
587 years for a given branch of Petaluridae on average. We inferred 49 high to low and low to high elevation
588 transitions each, averaging one of each transition every 14.5 million years for a given branch of
589 Petaluridae on average. The expected frequency of transitions per million years for a given branch of
590 Petaluridae did not change with *A. archangelskyi* removed.

591

592 **Discussion**

593 *Historical Island Geography Underlies a Species Complex*

594 As hypothesized, our results demonstrate that uplift and oceanic barriers have shaped the evolution of
595 Kapokapowai. The divergence time analysis suggested that the MRCA (2.6-15 Ma) of all sampled
596 Kapokapowai could very well have coincided with the accelerated tectonic uplift which occurred ~5Ma,
597 or the more gradual uplift from 10-5Ma (Fig. 1E). Intriguingly, a strong bottleneck in the ancestral
598 lineage of KS was identified between 2.5-10Ma from a reference genome (Tolman et al., 2023) using the
599 Pairwise Sequential Coalescent (PSMC; Liu & Hansen, 2017). This bottleneck could plausibly be
600 reflective of speciation between KM and KN+KS. KM has higher genetic diversity than either KN or KS
601 (Fig. 1A,B) supporting the hypothesis that this bottleneck was caused by a founder effect similar to many
602 other systems (Anopheles gambiae 1000 Genomes Consortium et al., 2017; Auton et al., 2015; B. Li et
603 al., 2024).

604 The genetic differentiation between KN and KS is much smaller than the differentiation between
605 either population and KM (Table 2). Although Te Moana o Raukawa (Cook Strait) is currently a barrier to
606 the dispersal of Kapokapowai, our species distribution models suggest that this has not always been the
607 case (Fig. 4, Supplemental Fig. 4). Perhaps Te Moana o Raukawa has not been a barrier to the dispersal
608 of Kapokapowai for a sufficient period of time for a strong genetic structure to evolve. On the other hand,
609 the peaks of Kā Tiritiri-o-te-Moana have not contained suitable habitat for KN or KS in any of the tested
610 time periods, and have likely served as a longer barrier to the dispersal of these populations, shaping the
611 genetic structure currently observed in Kapokapowai. The physical boundary of the mountains is further
612 compounded by the fact that the alpine habitat has shortened the flight season of KM, compared to KN
613 and KS (L. S. Wolfe, 1952).

614 The data we have here support a hypothesis in which all sampled Kapokapowai are descendants
615 of a population that colonized alpine habitats (the most supported pattern in the fauna of Aotearoa
616 (Buckley et al., 2024), although there is speculation that some lineages may have ridden tectonic uplift to
617 higher elevations (Heads, 2017)), while KN and KS descend from populations that later moved into
618 lowland habitats. Our ancestral state reconstruction analysis of Petaluridae would support the former, as
619 across 1000 simulations, transitions from high elevation to low and medium elevational maxims occurred
620 on average every 2.9 million years on each branch. It is entirely plausible that such flexibility in adjusting
621 to different elevations is a common trait in lineages that have persisted on Zealandia for tens of millions
622 of years. This hypothesis of recolonization of the lowlands is not without precedent, as plant lineages have
623 also been hypothesized to have colonized mountains, and then recolonized the lowlands of Aotearoa
624 (Thomas et al., 2023). A demographic model for KM from a reference genome, and revisiting the
625 specimens sampled here with genome-wide resequencing data could be used to generate a demographic
626 model for all populations of Kapokapowai, and a historical demographic model of dispersal and gene
627 flow between populations using the site-frequency-spectrum (Noskova et al., 2023), both of which could
628 be used to robustly test this hypothesis.

629

630 ***Gene Flow in the Presence of Geographic Barriers and Implications for Species Delimitation***

631 *Evidence of Current gene flow*

632 Despite the aforementioned geographic barriers, the PCA (Fig. 1A), admixture (Fig. 1B), and
633 introgression analyses all suggest there is some level of interbreeding and movement between
634 populations. Neither barrier seems to be entirely restricting gene flow, as evidenced by lower fixation (F_{ST}
635 < 0.30) than might be expected given > 5 million years of separation between KM and KN and KS (Fig.
636 1E), and evidence of introgression between KS and KM.

637 One individual KM notably inherited 75% of its ancestry from ancestral population one, which is
638 unique to KM, and 25% of its ancestry from ancestral population three (Fig. 1B). Thus, this individual is
639 likely the offspring of an F1-hybrid back-crossed with an individual with 100% of its ancestry from
640 population one, suggesting the genetic populations can breed with one another, and gene flow may still
641 occur in the present.

642

643 *Implications for species delimitation*

644 Given the dynamics of gene flow, current species delimitations in this complex are difficult to make.
645 Given the genetic differentiation between KM and KN and KS ($F_{ST} > .23$), our identification of a
646 diagnostic characteristic of the curvature on the horns of KM (Fig. 2), and the strong posterior support
647 (>99%) of the currently described species (*U. carovei* comprised of KN and KS and *U. chiltoni*
648 comprised of KM) in our species delimitation analysis, we suggest that current species delimitations
649 remain unchanged. Although KN and KS do show some genetic differentiation, they do not show
650 evidence of niche divergence, and we do not believe that they merit a new species description at this point
651 in time.

652

653 ***Generating Species Distribution Models for Island Species***

654 Although the utilization of GBIF occurrences in conjunction with genomic analyses provide the
655 opportunity for highly robust niche models which have the potential to match population admixture or
656 structuring among populations of odonates, a consequence is the underfitting of model performance due
657 to the abundance, range, and density of the species itself. ENM results for KN revealed low AUC values,

658 which is a continuous metric that provides discriminative ability in false positives and false negatives
659 (Phillips et al. 2017). Since KN is found throughout the entirety of Te Ika-a-Māui, our models were
660 unable to discern gradients of high and low suitability, resulting in poor model output. This pattern is also
661 observed in our AICc value (Supplementary Table S2). Our thinned dataset consisted of 239 occurrences,
662 sufficient to generate a robust model; the widespread distribution throughout Te Ika-a-Māui contributed
663 to high AICc scores.

664 ENMs in the context of island biogeography is an area of ongoing study, as model extrapolation
665 becomes poor for species endemic to small or singular islands (Sutherland et al. 2021, Goodman et al.
666 2024), limiting the incorporation of novel climatic conditions that could improve model fit. Furthermore
667 AUC values may be skewed if only a few climatic variables drive the model, leading to oversimplified
668 relationships with suitability (Phillips et al. 2017), as evidenced by the number of nonzero lambda
669 coefficients within our KN model (2)(See Supplementary Table S2).

670 Interestingly, our 10-percentile omission rate metrics were more robust (0.16). The 10-percentile
671 omission rate metric excludes the lowest 10 percent of raw occurrence values, thus creating a threshold
672 within suitability. Our lower omission rates suggest minimal outliers in our dataset, suggesting that our
673 predictions for KN on Te Ika-a-Māui are not overly generalist.

674 An aspect to consider in paleo-ecological modeling (PaleoENM) is the use of multiple lines of
675 evidence to assess model fidelity. Incorporating supplemental analyses such as response curves and
676 ordination analyses provide clarity to model over- or under-extrapolation, which can be interpreted as
677 either model error or accuracy. Response curves demonstrate if the full environmental range of the
678 species has been sampled for each species or population, while ordination analyses allow
679 multidimensional visualization of the niche outside of a spatial context. In the case of our data, response
680 curves, albeit jagged, map the full relationship of each climatic variable within the model, while our
681 ordination analysis demonstrates statistical differences among the KN and KS populations. Overall,
682 although genetic divergence was low among KN and KS populations, the ecological and distributional
683 differences among both populations are the result in differences in climatic conditions, and not a result of
684 poor model performance because of inappropriate *a priori* grouping of populations based on their presence
685 on Te Ika-a-Māui or Te Waipounamu.

686

687 Conclusion

688 To look at species diversity and the potential for speciation in a “relict” group such as the petaltail
689 dragonflies offers a unique perspective in evolutionary biology, as well as island ecology. Analyses
690 suggest that this family is extremely old, even for an order as ancient as Odonata, with some extant
691 species persisting as independent evolutionary lineages since the Cretaceous era (Kohli et al., 2021;
692 Suvorov et al., 2022; E. R. Tolman et al., 2024). With their reliance on fen habitats, Petaluridae are also
693 somewhat limited in their range, compared to more generalist dragonflies that use ponds or rivers to
694 complete their life cycle. Despite this, our results demonstrate that speciation in Petaluridae is associated
695 with shifts to habitats at different elevations, in both Kapokapowai and other groups of petaltails, which
696 may be associated with their long persistence. While species of Kapokapowai have potentially been
697 separated for significant periods of time, either across islands or in different habitats within an island, it
698 may be that their adaptations to these specialized fen habitats has limited the genetic variability that
699 would lead to speciation. This may help to explain why this group, despite its age, continues to be the
700 smallest family within Anisoptera.

701

702 **References**

703 Andress, R. (1998). *Description of the larva of Petalura ingentissima Tillyard, 1907 (Anisoptera: Petaluridae)*. <http://archive.org/details/odonatologica-27-353-359>

704 Anopheles gambiae 1000 Genomes Consortium, Data analysis group, Partner working group, Sample collections—Angola:, Burkina Faso:, Cameroon:, Gabon:, Guinea:, Guinea-Bissau:, Kenya:, Uganda:, Crosses:, Sequencing and data production, Web application development, & Project coordination. (2017). Genetic diversity of the African malaria vector Anopheles gambiae. *Nature*, 552(7683), 96–100. <https://doi.org/10.1038/nature24995>

705 Auton, A., Abecasis, G. R., Altshuler, D. M., Durbin, R. M., Abecasis, G. R., Bentley, D. R., Chakravarti, A., Clark, A. G., Donnelly, P., Eichler, E. E., Flicek, P., Gabriel, S. B., Gibbs, R. A., Green, E. D., Hurles, M. E., Knoppers, B. M., Korbel, J. O., Lander, E. S., Lee, C., ... National Eye Institute, N. (2015). A global reference for human genetic variation. *Nature*, 526(7571), 68–74. <https://doi.org/10.1038/nature15393>

706 Barreto, E., Rangel, T. F., Pellissier, L., & Graham, C. H. (2021). Area, isolation and climate explain the diversity of mammals on islands worldwide. *Proceedings of the Royal Society B: Biological Sciences*, 288(1965), 20211879. <https://doi.org/10.1098/rspb.2021.1879>

707 Bercovich, U., M. S. Rasmussen, Z. Li, C. Wiuf, and A. Albrechtsen. 2025. Measuring linkage disequilibrium and improvement of pruning and clumping in structured populations. *Genetics* 229:iyaf009.

708 Booth, T. H. (2022). Checking bioclimatic variables that combine temperature and precipitation data before their use in species distribution models. *Austral Ecology*, 47(7), 1506–1514. <https://doi.org/10.1111/aec.13234>

709 Bouckaert, R., Heled, J., Kühnert, D., Vaughan, T., Wu, C.-H., Xie, D., Suchard, M. A., Rambaut, A., & Drummond, A. J. (2014). BEAST 2: A Software Platform for Bayesian Evolutionary Analysis. *PLOS Computational Biology*, 10(4), e1003537. <https://doi.org/10.1371/journal.pcbi.1003537>

710 Bouckaert, R. R. (2022). An Efficient Coalescent Epoch Model for Bayesian Phylogenetic Inference. *Systematic Biology*, 71(6), 1549–1560. <https://doi.org/10.1093/sysbio/syac015>

711 Brown, J. L., Hill, D. J., Dolan, A. M., Carnaval, A. C., & Haywood, A. M. (2018). PaleoClim, high spatial resolution paleoclimate surfaces for global land areas. *Scientific Data*, 5(1), Article 1. <https://doi.org/10.1038/sdata.2018.254>

712 Buckley, T. R., Hoare, R. J. B., & Leschen, R. A. B. (2024). Key questions on the evolution and biogeography of New Zealand alpine insects. *Journal of the Royal Society of New Zealand*, 54(1), 30–54. <https://doi.org/10.1080/03036758.2022.2130367>

713 Cairns, J., I. R. C. Baird, F. Johnson, L. Noble, and W. Glamore. 2025. Detecting \square : Novel eDNA Method and Water Balance Modelling Insights Enable Improved Catchment Management and Conservation Outcomes. *Ecohydrology* 18:e70013.

714 Conway, M., & Olsen, B. J. (2019). Contrasting drivers of diversification rates on islands and continents across three passerine families. *Proceedings. Biological Sciences*, 286(1915), 20191757. <https://doi.org/10.1098/rspb.2019.1757>

715 Córdoba-Aguilar, A., Beatty, C. D., & Bried, J. T. (2022). Introduction to Dragonflies and Damselflies, Second Edition. In A. Córdoba-Aguilar, C. Beatty, & J. Bried (Eds.), *Dragonflies and Damselflies: Model Organisms for Ecological and Evolutionary Research* (p. 0). Oxford University Press. <https://doi.org/10.1093/oso/9780192898623.003.0001>

716 Cooper, A., and R. A. Cooper. 1997. The Oligocene bottleneck and New Zealand biota: genetic record of a past environmental crisis. *Proceedings of the Royal Society of London. Series B: Biological Sciences* 261:293–302. Royal Society.

717 Danecek, P., Bonfield, J. K., Liddle, J., Marshall, J., Ohan, V., Pollard, M. O., Whitwham, A., Keane, T., McCarthy, S. A., Davies, R. M., & Li, H. (2021). Twelve years of SAMtools and BCFtools. *GigaScience*, 10(2), giab008. <https://doi.org/10.1093/gigascience/giab008>

752 Di Cola, V., Broennimann, O., Petitpierre, B., Breiner, F. T., D'Amen, M., Randin, C., Engler, R., Pottier,
753 J., Pio, D., Dubuis, A., Pellissier, L., Mateo, R. G., Hordijk, W., Salamin, N., & Guisan, A.
754 (2017). ecospat: An R package to support spatial analyses and modeling of species niches and
755 distributions. *Ecography*, 40(6), 774–787. <https://doi.org/10.1111/ecog.02671>

756 Douglas, J., & Bouckaert, R. (2022). Quantitatively defining species boundaries with more efficiency and
757 more biological realism. *Communications Biology*, 5(1), 1–10. <https://doi.org/10.1038/s42003-022-03723-z>

758 Dray, S., & Dufour, A.-B. (2007). The ade4 Package: Implementing the Duality Diagram for Ecologists.
759 *Journal of Statistical Software*, 22, 1–20. <https://doi.org/10.18637/jss.v022.i04>

760 Durrant, R. (2024). *Invertebrate Justice: Extending The Boundaries of Non-Speciesist Green
761 Criminology*. Springer Nature.

762 Fick, S. E., & Hijmans, R. J. (2017). WorldClim 2: New 1-km spatial resolution climate surfaces for
763 global land areas. *International Journal of Climatology*, 37(12), 4302–4315.
764 <https://doi.org/10.1002/joc.5086>

765 Fong, H. M. (2024). *A revision of the genus Mecodema Blanchard 1853 (Coleoptera: Carabidae) species
766 groups ducale and laterale from the South Island, Aotearoa New Zealand* [Thesis,
767 ResearchSpace@Auckland]. <https://researchspace.auckland.ac.nz/handle/2292/70309>

768 GBIF.org (1 May 2025) GBIF Occurrence Download <https://doi.org/10.15468/dl.t648we>

769 Gleditsch, J., Behm, J., Ellers, J., Jesse, W., & Helmus, M. (2022). *Contemporizing island biogeography
770 theory with anthropogenic drivers of species richness*.
<https://doi.org/10.22541/au.163955172.21711050/v3>

771 Goodman, A., Tolman, E., Uche-Dike, R., Abbott, J., Breinholt, J. W., Bybee, S., Frandsen, P. B.,
772 Gosnell, J. S., Guralnick, R., Kalkman, V. J., Kohli, M., Lontchi, J. F., Lupiyaningdyah, P.,
773 Newton, L., & Ware, J. L. (2023). Assessment of targeted enrichment locus capture across time
774 and museums using odonate specimens. *Insect Systematics and Diversity*, 7(3), 5.
775 <https://doi.org/10.1093/isd/ixad011>

776 Goodman, A. M., Beatty, C. D., Bütse, S., Ubukata, H., Miyazaki, T., Blair, M. E., & Ware, J. L. (2024).
777 Paleoecological niche modeling of Epiophlebia (Epiophlebiptera: Epiophlebiidae) reveals
778 continuous distribution during the Last Glacial Maximum. *International Journal of Odonatology*,
779 27, 60–76. <https://doi.org/10.48156/1388.2024.1917262>

780 Grandcolas, P., R. Nattier, and S. Trewick. 2014. Relict species: a relict concept? Trends in
781 Ecology & Evolution 29:655–663.

782 Grant, E. A. (2014). *Bronze as a non-custodial intervention in the interpretation of insects from the
783 natural world of Māori: An exhibition report presented in partial fulfilment of the requirements
784 for the degree of Doctor of Philosophy in Fine Arts at Massey University, Palmerston North,
785 Aotearoa, New Zealand* [Massey University]. <http://hdl.handle.net/10179/6512>

786 Harris, C. R., Millman, K. J., Van Der Walt, S. J., Gommers, R., Virtanen, P., Cournapeau, D., Wieser,
787 E., Taylor, J., Berg, S., Smith, N. J., Kern, R., Picus, M., Hoyer, S., Van Kerkwijk, M. H., Brett,
788 M., Haldane, A., Del Río, J. F., Wiebe, M., Peterson, P., ... Oliphant, T. E. (2020). Array
789 programming with NumPy. *Nature*, 585(7825), 357–362. <https://doi.org/10.1038/s41586-020-2649-2>

790 Heads, M. J. (2017). *Biogeography and evolution in New Zealand*. CRC press, Taylor & Francis group.

791 Hijmans R (2025). *raster: Geographic Data Analysis and Modeling*. R package version 3.6-32,
792 <https://github.com/rspatial/raster>.

793 Hollister, J., T. Shah, J. Nowosad, A. L. Robitaille, M. W. Beck, and M. Johnson. 2023. elevatr:
794 Access Elevation Data from Various APIs.

795 Jenkins, T. L. (2024). mapmixture: An R package and web app for spatial visualisation of admixture and
796 population structure. *Molecular Ecology Resources*, e13943. <https://doi.org/10.1111/1755-0998.13943>

801 Jessen, T. D., N. C. Ban, N. X. Claxton, and C. T. Darimont. 2022. Contributions of Indigenous
802 Knowledge to ecological and evolutionary understanding. *Frontiers in Ecology and the*
803 *Environment* 20:93–101.

804 Jones, L. A., W. Gearty, B. J. Allen, K. Eichenseer, C. D. Dean, S. Galván, M. Kouvari, P. L.
805 Godoy, C. S. C. Nicholl, L. Buffan, E. M. Dillon, J. T. Flannery-Sutherland, and A. A. Chiarenza.
806 2023. palaeoverse: A community-driven R package to support palaeobiological analysis. *Methods*
807 in *Ecology and Evolution* 14:2205–2215

808 Karger, D. N., Conrad, O., Böhner, J., Kawohl, T., Kreft, H., Soria-Auza, R. W., Zimmermann, N. E.,
809 Linder, H. P., & Kessler, M. (2017). Climatologies at high resolution for the earth's land surface
810 areas. *Scientific Data*, 4(1), Article 1. <https://doi.org/10.1038/sdata.2017.122>

811 Karger, D. N., Nobis, M. P., Normand, S., Graham, C. H., & Zimmermann, N. E. (2023). CHELSA-
812 TraCE21k – high-resolution (1 km) downscaled transient temperature and precipitation
813 data since the Last Glacial Maximum. *Climate of the Past*, 19(2), 439–456.
814 <https://doi.org/10.5194/cp-19-439-2023>

815 Kass, J. M., Muscarella, R., Galante, P. J., Bohl, C. L., Pinilla-Buitrago, G. E., Boria, R. A., Soley-
816 Guardia, M., & Anderson, R. P. (2021). ENMeval 2.0: Redesigned for customizable and
817 reproducible modeling of species' niches and distributions. *Methods in Ecology and Evolution*,
818 12(9), 1602–1608. <https://doi.org/10.1111/2041-210X.13628>

819 Kass, J. M., Vilela, B., Aiello-Lammens, M. E., Muscarella, R., Merow, C., & Anderson, R. P. (2018).
820 Wallace: A flexible platform for reproducible modeling of species niches and distributions built
821 for community expansion. *Methods in Ecology and Evolution*, 9(4), 1151–1156.
822 <https://doi.org/10.1111/2041-210X.12945>

823 Kennedy, C. H. (1922). The morphology of the penis in the genus *Libellula* (Odonata). *Entomology*
824 *Newsletter*, 33, 33–40.

825 Kohli, M., Letsch, H., Greve, C., Béthoux, O., Deregnaucourt, I., Liu, S., Zhou, X., Donath, A., Mayer,
826 C., Podsiadlowski, L., Gunkel, S., Machida, R., Niehuis, O., Rust, J., Wappler, T., Yu, X., Misof,
827 B., & Ware, J. (2021). Evolutionary history and divergence times of Odonata (dragonflies and
828 damselflies) revealed through transcriptomics. *iScience*, 24(11), 103324.
829 <https://doi.org/10.1016/j.isci.2021.103324>

830 Kuznetsova, V. G., & Golub, N. V. (2020). A checklist of chromosome numbers and a review of
831 karyotype variation in Odonata of the world. *Comparative Cytogenetics*, 14(4), 501–540.
832 <https://doi.org/10.3897/CompCytogen.v14i4.57062>

833 L. S. Wolfe. (1952). A study of the genus *Uropetala* Selys (Order Odonata) from New Zealand.
834 *Transactions of the Royal Society of New Zealand*, 80, 245–275.

835 Leschen, R., Collier, K., Death, R., Harding, J., & Smith, B. (2023). Systematics expertise and taxonomic
836 status of New Zealand's freshwater insects. *New Zealand Science Review*, 73(3–4), 92–95.
837 <https://doi.org/10.26686/nzsr.v73i3-4.8534>

838 Lewis, K. B., Carter, L., & Davey, F. J. (1994). The opening of Cook Strait: Interglacial tidal scour and
839 aligning basins at a subduction to transform plate edge. *Marine Geology*, 116(3), 293–312.
840 [https://doi.org/10.1016/0025-3227\(94\)90047-7](https://doi.org/10.1016/0025-3227(94)90047-7)

841 Li, B., Duan, Y., Du, Z., Wang, X., Liu, S., Feng, Z., Tian, L., Song, F., Yang, H., Cai, W., Lin, Z., & Li,
842 H. (2024). Natural selection and genetic diversity maintenance in a parasitic wasp during
843 continuous biological control application. *Nature Communications*, 15(1), 1379.
844 <https://doi.org/10.1038/s41467-024-45631-2>

845 Li, H., & Durbin, R. (2009). Fast and accurate short read alignment with Burrows–Wheeler transform.
846 *Bioinformatics*, 25(14), 1754–1760. <https://doi.org/10.1093/bioinformatics/btp324>

847 Liu, S., & Hansen, M. M. (2017). PSMC (pairwise sequentially Markovian coalescent) analysis of RAD
848 (restriction site associated DNA) sequencing data. *Molecular Ecology Resources*, 17(4), 631–641.
849 <https://doi.org/10.1111/1755-0998.12606>

850 Lobo, J. M., Jiménez-Valverde, A., & Real, R. (2008). AUC: A misleading measure of the performance
851 of predictive distribution models. *Global Ecology and Biogeography*, 17(2), 145–151.
852 <https://doi.org/10.1111/j.1466-8238.2007.00358.x>

853 Malinsky, M., Matschiner, M., & Svardal, H. (2021). Dsuite—Fast D-statistics and related admixture
854 evidence from VCF files. *Molecular Ecology Resources*, 21(2), 584–595.
855 <https://doi.org/10.1111/1755-0998.13265>

856 May, M. L. (1997). Reconsideration of the status of the genera *Phyllomacromia* and *Macromia*
857 (Anisoptera: Corduliidae). *Odonatologica*, 26(4), 405–414.

858 McCulloch, G. A., and J. M. Waters. 2019. Phylogenetic divergence of island biotas: Molecular
859 dates, extinction, and “relict” lineages. *Molecular Ecology* 28:4354–4362.

860 McKinney, W. (2010). *Data Structures for Statistical Computing in Python*. 56–61.
861 <https://doi.org/10.25080/Majora-92bf1922-00a>

862 Naimi, B. (2023). *usdm: Uncertainty Analysis for Species Distribution Models* (Version 2.1-6) [Computer
863 software]. <https://cran.r-project.org/web/packages/usdm/index.html>

864 Noskova, E., Abramov, N., Iliutkin, S., Sidorin, A., Dobrynin, P., & Ulyantsev, V. (2023). *GADM42:*
865 *More efficient and flexible demographic inference from genetic data* (p. 2022.06.14.496083).
866 bioRxiv. <https://doi.org/10.1101/2022.06.14.496083>

867 Oksanen, J., Simpson, G. L., Blanchet, F. G., Kindt, R., Legendre, P., Minchin, P. R., O’Hara, R. B.,
868 Solymos, P., Stevens, M. H. H., Szoechs, E., Wagner, H., Barbour, M., Bedward, M., Bolker, B.,
869 Borcard, D., Carvalho, G., Chirico, M., Caceres, M. D., Durand, S., ... Weedon, J. (2024). *vegan:*
870 *Community Ecology Package* (Version 2.6-6.1) [Computer software]. <https://cran.r-project.org/web/packages/vegan/index.html>

871 O’Neill, S. B., Chapple, D. G., Daugherty, C. H., & Ritchie, P. A. (2008). Phylogeography of two New
872 Zealand lizards: McCann’s skink (*Oligosoma maccanni*) and the brown skink (*O. zealandicum*).
873 *Molecular Phylogenetics and Evolution*, 48(3), 1168–1177.
874 <https://doi.org/10.1016/j.ympev.2008.05.008>

875 Peterson, A. T., & Lieberman, B. S. (2012). Species’ Geographic Distributions Through Time: Playing
876 Catch-up with Changing Climates. *Evolution: Education and Outreach*, 5(4), 569–581.
877 <https://doi.org/10.1007/s12052-012-0385-2>

878 Phillips, S. J., Anderson, R. P., Dudik, M., Schapire, R. E., & Blair, M. E. (2017). Opening the black box:
879 An open-source release of Maxent. *Ecography*, 40(7), 887–893.
880 <https://doi.org/10.1111/ecog.03049>

881 Purcell, S., Neale, B., Todd-Brown, K., Thomas, L., Ferreira, M. A. R., Bender, D., Maller, J., Sklar, P.,
882 de Bakker, P. I. W., Daly, M. J., & Sham, P. C. (2007). PLINK: A Tool Set for Whole-Genome
883 Association and Population-Based Linkage Analyses. *American Journal of Human Genetics*,
884 81(3), 559–575.

885 Radosavljevic, A., & Anderson, R. P. (2014). Making better Maxent models of species distributions:
886 Complexity, overfitting and evaluation. *Journal of Biogeography*, 41(4), 629–643.
887 <https://doi.org/10.1111/jbi.12227>

888 Rambaut, A., Drummond, A. J., Xie, D., Baele, G., & Suchard, M. A. (2018). Posterior Summarization in
889 Bayesian Phylogenetics Using Tracer 1.7. *Systematic Biology*, 67(5), 901–904.
890 <https://doi.org/10.1093/sysbio/syy032>

891 Revell, L. J. 2012. phytools: an R package for phylogenetic comparative biology (and other
892 things). *Methods in Ecology and Evolution* 3:217–223.

893 R Core Team. 2021. R: A language and environment for statistical computing. R Foundation for
894 Statistical Computing, Vienna, Austria.

895 Schoener, T. W. (1968). The Anolis Lizards of Bimini: Resource Partitioning in a Complex Fauna.
896 *Ecology*, 49(4), 704–726. <https://doi.org/10.2307/1935534>

897 Shepherd, L., Simon, C., Langton-Myers, S., & Morgan-Richards, M. (2024). Insights into Aotearoa New
898 Zealand’s biogeographic history provided by the study of natural hybrid zones. *Journal of the*
899 *Royal Society of New Zealand*, 54(1), 55–74. <https://doi.org/10.1080/03036758.2022.2061020>

901 Skotte, L., Korneliussen, T. S., & Albrechtsen, A. (2013). Estimating individual admixture proportions
902 from next generation sequencing data. *Genetics*, 195(3), 693–702.
903 <https://doi.org/10.1534/genetics.113.154138>

904 Scotese, C. R., and N. M. Wright. 2018. PALEOMAP Paleodigital Elevation Models
905 (PaleoDEMS) for the Phanerozoic. Zenodo.

906 Stevens, M. I., & Hogg, I. D. (2004). Population genetic structure of New Zealand's endemic corophiid
907 amphipods: Evidence for allopatric speciation. *Biological Journal of the Linnean Society*, 81(1),
908 119–133. <https://doi.org/10.1111/j.1095-8312.2004.00270.x>

909 Stoltz, M., Baeumer, B., Bouckaert, R., Fox, C., Hiscox, G., & Bryant, D. (2021). Bayesian Inference of
910 Species Trees using Diffusion Models. *Systematic Biology*, 70(1), 145–161.
911 <https://doi.org/10.1093/sysbio/syaa051>

912 Sutherland, L. N., G. S. Powell, and S. M. Bybee. 2021. Validating species distribution models to
913 illuminate coastal fireflies in the South Pacific (Coleoptera: Lampyridae). *Sci. Rep.* 11: 17397.

914 Suvorov, A., Scornavacca, C., Fujimoto, M. S., Bodily, P., Clement, M., Crandall, K. A., Whiting, M. F.,
915 Schrider, D. R., & Bybee, S. M. (2022). Deep Ancestral Introgression Shapes Evolutionary
916 History of Dragonflies and Damselflies. *Systematic Biology*, 71(3), 526–546.
917 <https://doi.org/10.1093/sysbio/syab063>

918 Taylor, R. (1855). *Te Ika a Maui, or, New Zealand and its inhabitants: With the geology, natural history,
919 productions, and climate of the country, &c* (Vol. 1855, pp. 1–554).
920 <https://doi.org/10.5962/bhl.title.161768>

921 Taylor, R. (with Smithsonian Libraries). (1870). *Te Ika a Māui, or, New Zealand and its inhabitants:
922 Illustrating the origin, manners, customs, mythology, religion, rites, songs, proverbs, fables and
923 language of the Māori and Polynesian races in general*; together with the geology, natural
924 history, productions, and climate of the country. London: William Macintosh; Wanganui,
925 N.Z.: H. Ireson Jones. <http://archive.org/details/teikamauiornewze00tayl>

926 Thomas, A., Meudt, H. M., Larcombe, M. J., Igea, J., Lee, W. G., Antonelli, A., & Tanentzap, A. J.
927 (2023). Multiple origins of mountain biodiversity in New Zealand's largest plant radiation.
928 *Journal of Biogeography*, 50(5), 947–960. <https://doi.org/10.1111/jbi.14589>

929 Tolman, E. R., Beatty, C. D., Frandsen, P. B., Bush, J., Bruchim, O. R., Driever, E. S., Harding, K. M.,
930 Jordan, D., Kohli, M. K., Park, J., Park, S., Reyes, K., Rosari, M., Ryu, J. L., Wade, V., & Ware,
931 J. L. (2023). *Newly Sequenced Genomes Reveal Patterns of Gene Family Expansion in select
932 Dragonflies (Odonata: Anisoptera)* (p. 2023.12.11.569651). bioRxiv.
933 <https://doi.org/10.1101/2023.12.11.569651>

934 Tolman, E. R., Beatty, C. D., Kohli, M. K., Abbott, J., Bybee, S. M., Frandsen, P. B., Stephen Gosnell, J.,
935 Guralnick, R., Kalkman, V. J., Newton, L. G., Suvorov, A., & Ware, J. L. (2024). A molecular
936 phylogeny of the Petaluridae (Odonata: Anisoptera): A 160-Million-Year-Old story of drift and
937 extinction. *Molecular Phylogenetics and Evolution*, 200, 108185.
938 <https://doi.org/10.1016/j.ympev.2024.108185>

939 Trewick, S. A., Pilkington, S., Shepherd, L. D., Gibb, G. C., & Morgan-Richards, M. (2017). Closing the
940 gap: Avian lineage splits at a young, narrow seaway imply a protracted history of mixed
941 population response. *Molecular Ecology*, 26(20), 5752–5772. <https://doi.org/10.1111/mec.14323>

942 Veloz, S. D. (2009). Spatially autocorrelated sampling falsely inflates measures of accuracy for presence-
943 only niche models. *Journal of Biogeography*, 36(12), 2290–2299. [https://doi.org/10.1111/j.1365-2699.2009.02174.x](https://doi.org/10.1111/j.1365-
944 2699.2009.02174.x)

945 W. J. Winstanley. (1981). AN EMERGENCE STUDY ON UROPETALA CAROEI CAROEI
946 (ODONATA: PETALURIDAE) NEAR WELLINGTON, NEW ZEALAND, WITH NOTES ON
947 THE BEHAVIOUR OF THE SUBSPECIES. *Tuatara*, 25(1).

948 Wallis, G. P., & Buckley, T. R. (2024). Evolutionary biogeography of Aotearoa. *Journal of the Royal
949 Society of New Zealand*, 54(1), 1–7. <https://doi.org/10.1080/03036758.2023.2260539>

950 Ware, J. L. (2008). *MOLECULAR AND MORPHOLOGICAL SYSTEMATICS OF LIBELLULOIDEA*
951 (*ODONATA: ANISOPTERA*) AND *DICTYOPTERA* [PhD Thesis, Rutgers University].
952 <https://rucore.libraries.rutgers.edu/rutgers-lib/24985/PDF/1>

953 Ware, J. L., Beatty, C. D., Herrera, M. S., Valley, S., Johnson, J., Kerst, C., May, M. L., & Theischinger,
954 G. (2014). The petaltail dragonflies (Odonata: Petaluridae): Mesozoic habitat specialists that
955 survive to the modern day. *Journal of Biogeography*, 41(7), 1291–1300.
956 <https://doi.org/10.1111/jbi.12273>

957 Warren, D. L., & Seifert, S. N. (2011). Ecological niche modeling in Maxent: The importance of model
958 complexity and the performance of model selection criteria. *Ecological Applications*, 21(2), 335–
959 342. <https://doi.org/10.1890/10-1171.1>

960 Waters, J. M., & Craw, D. (2006). Goodbye Gondwana? New Zealand Biogeography, Geology, and the
961 Problem of Circularity. *Systematic Biology*, 55(2), 351–356.
962 <https://doi.org/10.1080/10635150600681659>

963 Wilson, E. O. (2009). Island Biogeography in the 1960s: Theory and Experiment. In *The Theory of Island*
964 *Biogeography Revisited* (pp. 1–12). Princeton University Press.
965 <https://doi.org/10.1515/9781400831920.1>

966 Winstanley, W. J., & Rowe, R. J. (1980). The larval habitat of *Uropetala carovei carovei* (Odonata:
967 Petaluridae) in the North Island of New Zealand, and the geographical limits of the subspecies.
968 *New Zealand Journal of Zoology*, 7(1), 127–134.
969 <https://doi.org/10.1080/03014223.1980.10423769>

970 Wyckhuys, K. A. G., Sanchez Garcia, F. J., Santos, A. M. C., Canal, N. A., Furlong, M. J., Melo, M. C.,
971 Gc, Y. D., & Pozsgai, G. (2022). Island and Mountain Ecosystems as Testbeds for Biological
972 Control in the Anthropocene. *Frontiers in Ecology and Evolution*, 10.
973 <https://doi.org/10.3389/fevo.2022.912628>

974

Table 1: Reference table of colonial and Māori names of localities and taxa.

| Geographic localities | |
|-------------------------------|--|
| <u>Māori name</u> | <u>Colonial name</u> |
| Aotearoa | New Zealand |
| Te Moana o Raukawa | Cook Strait |
| Te Ika-a-Māui | North Island |
| Te Waipounamu | South Island |
| Kā Tiritiri-o-te-Moana | Southern Alps |
| Population Names | |
| Māori names used in this work | Scientific name and locality |
| Kapokapowai North (KN) | <i>Uropetala carovei</i> , Te Ika-a-Māui |

| | |
|--------------------------|---|
| Kapokapowai South (KS) | <i>Uropetala carovei</i> , Te Waipounamu (below 1.2 km) |
| Kapokapowai Montane (KM) | <i>Uropetala chiltoni</i> , Kā Tiritiri-o-te-Moana |

975

976

Table 2: F_{ST} values between putative species of Kapokapowai, using 365 called SNPs. Kapokapowai North (KN), Kapokapowai Montane (KM), and Kapokapowai South (KS) are abbreviated. The results show stronger segmentation between KM and KN and KS.

| Pairwise comparison | Mean F _{ST} | Weighted F _{ST} |
|---------------------|----------------------|--------------------------|
| KM-KS | 0.20 | 0.23 |
| KM-KN | 0.27 | 0.29 |
| KN-KS | 0.05 | 0.11 |

977

978

Table 3: gene flow between Populations of Kapokapowai

| P1 | P2 | P3 | Dstatistic | Z-score | p-value | f4-ratio | BBAA | ABBA | BABA |
|----|----|----|------------|---------|---------|----------|-------|-------|-------|
| KN | KS | KM | 0.15 | 3.74 | < 0.01 | 0.08 | 25.89 | 28.52 | 20.86 |

Table 3: ABBA-BABA test output generated with Dsuite provides evidence of gene flow between KN and KS, as variants shared by KS and KM are significantly more common than variants shared by KM and KN ($p < 0.01$).

979

980

Table 4: PCA loadings, importance of variables, percent overlap, percent of unique niche overlap from both islands, environmental similarity (Schoener's D), and results of similarity tests from our EcoSpat analyses.

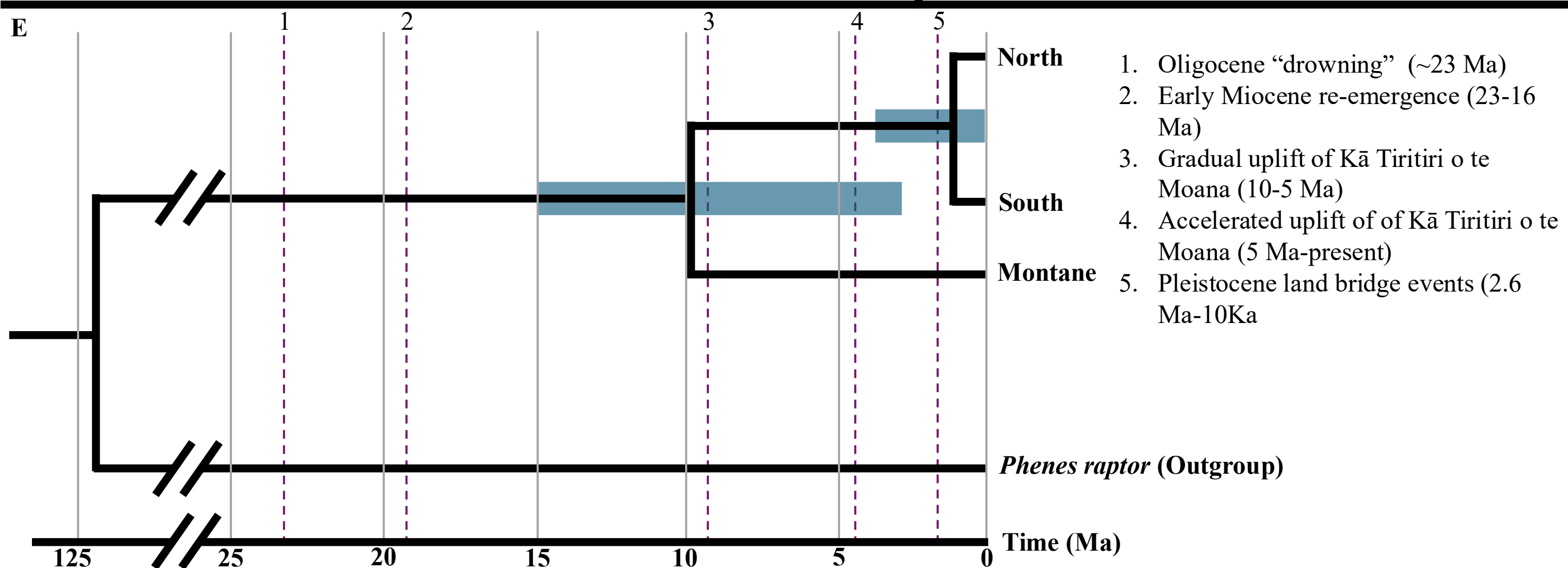
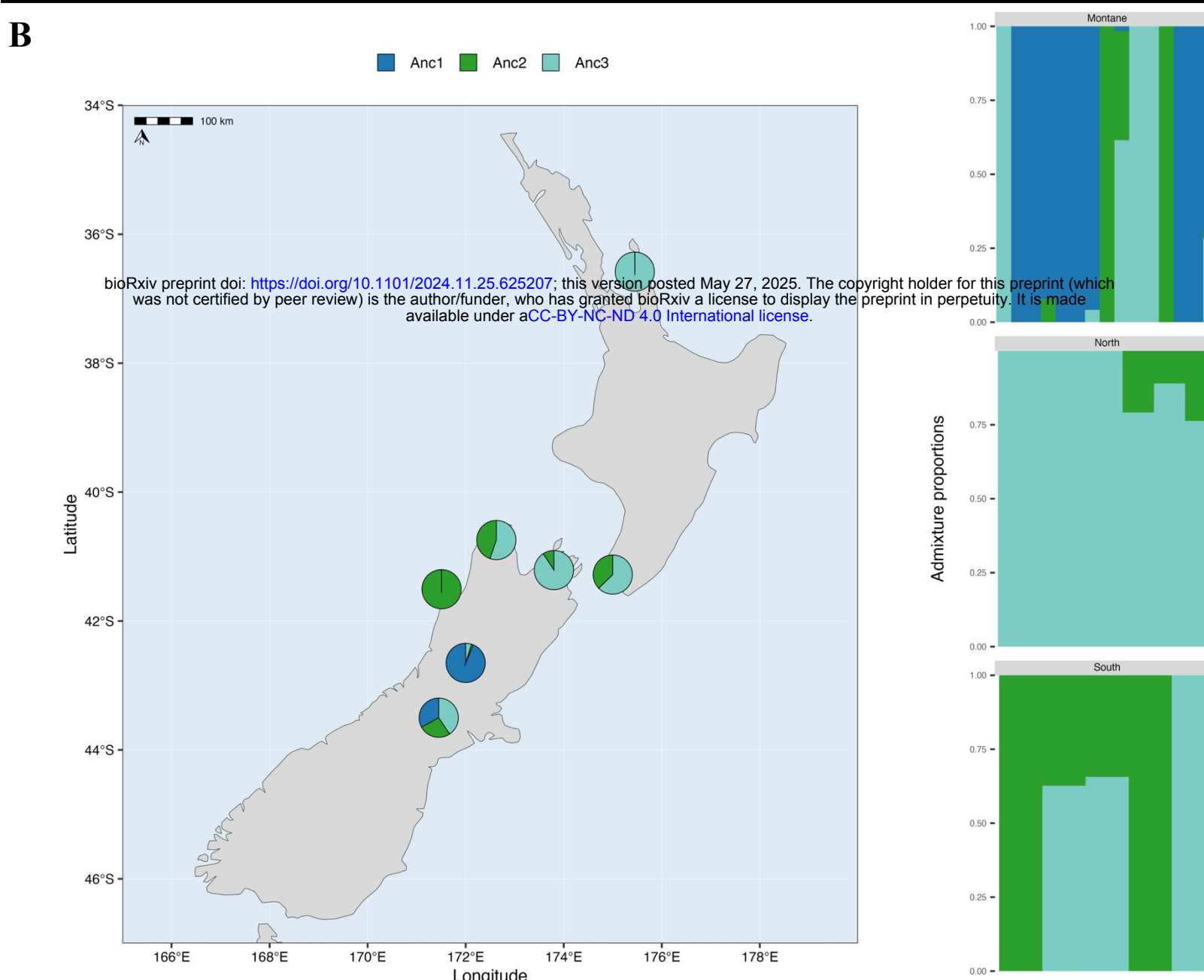
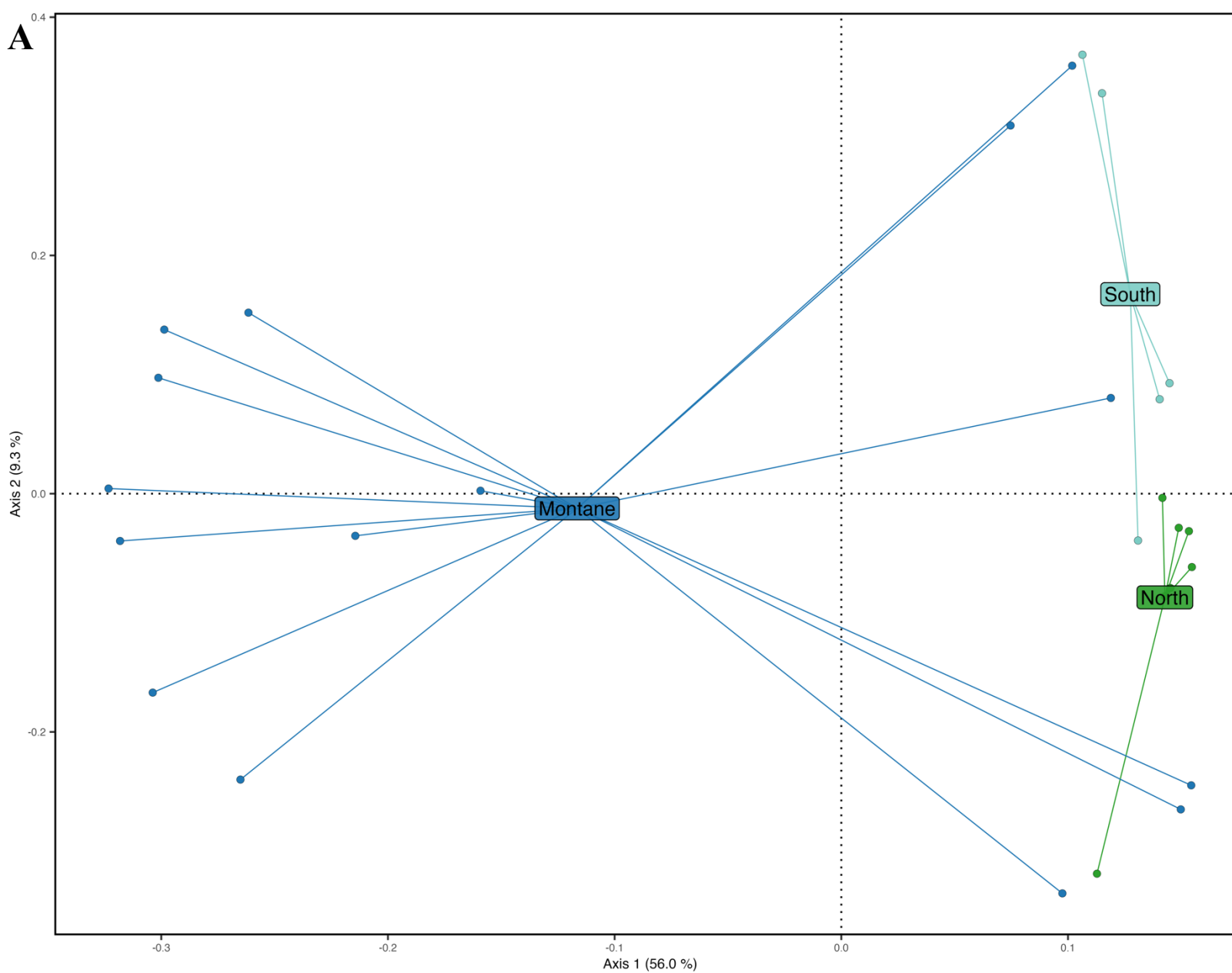
| Species | PC1 | PC2 | Overlap (%) | Unique North Island (%) | Unique South Island (%) | Schoener' s D | Similarit y test (p) |
|--------------------------------------|-------------|-------------|-------------|-------------------------|-------------------------|---------------|----------------------|
| Kapokapowai (North and South) | 34.9 | 32.6 | 93 | 6.9 | 13.2 | 24.7 | 0.01 |

Environmental PC1 PC2 PC3

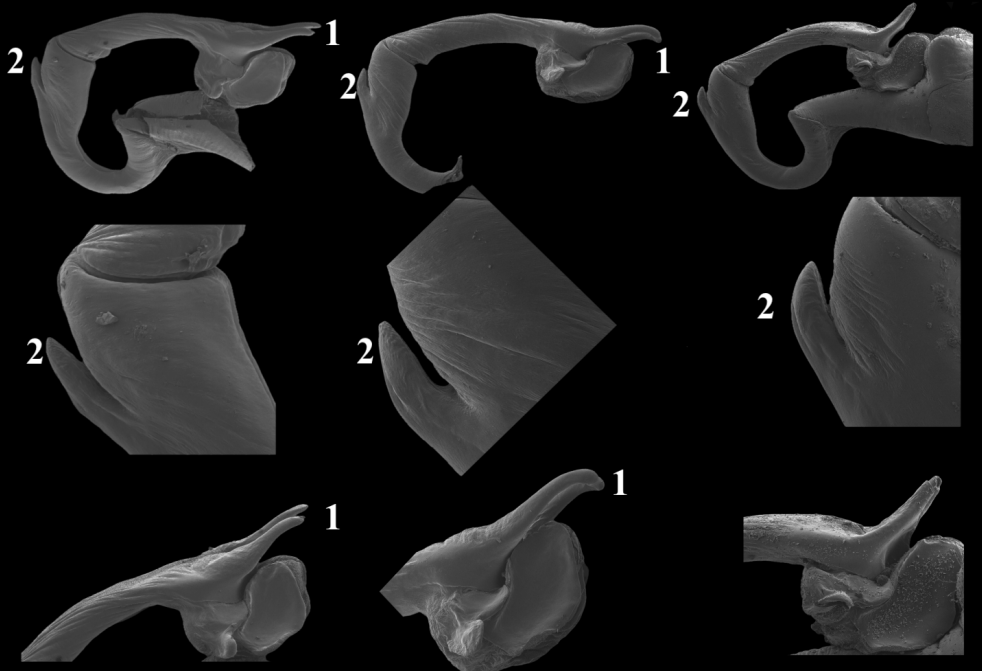
Variable

| | | | |
|---------------|--------------|--------------|--------------|
| bio 3 | -0.51 | -0.27 | -0.38 |
| bio 4 | -0.51 | -0.17 | -0.48 |
| bio 5 | 0.11 | 0.47 | -0.54 |
| bio 15 | 0.24 | 0.49 | -0.37 |
| bio 18 | 0.38 | -0.56 | -0.20 |
| bio 19 | 0.51 | -0.35 | -0.40 |

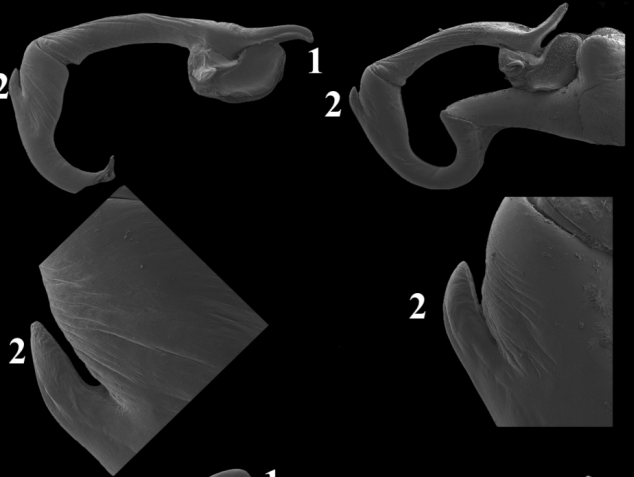
981



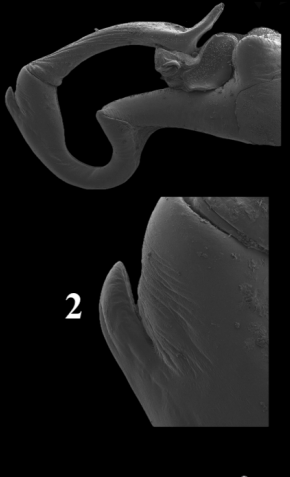
**Kapokapowai
Montane**



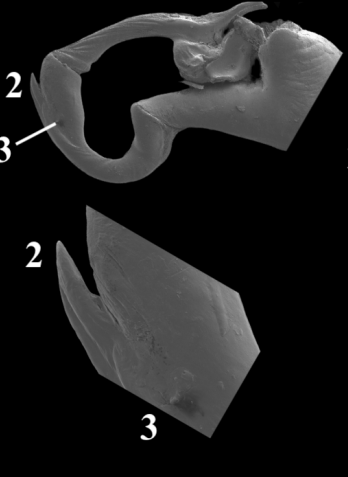
**Kapokapowai
Montane**



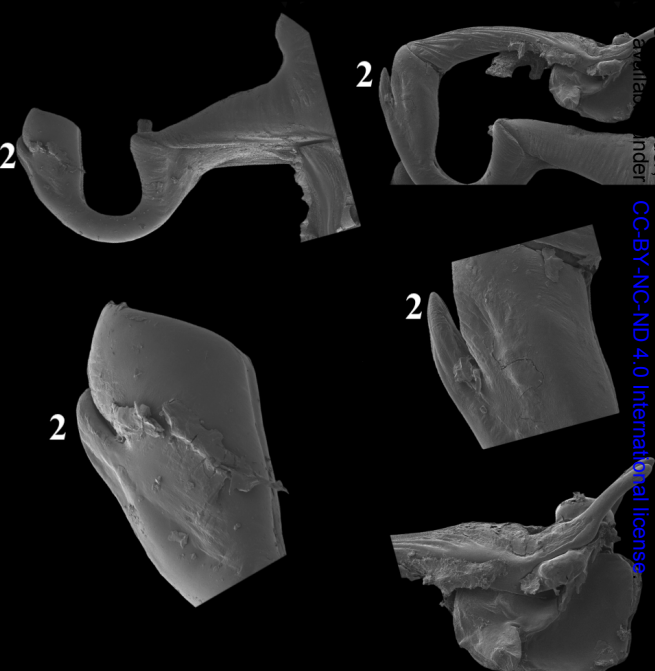
**Kapokapowai
North**



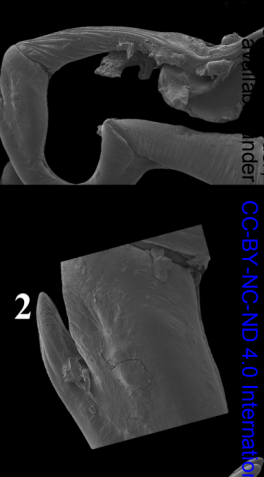
**Kapokapowai
North**

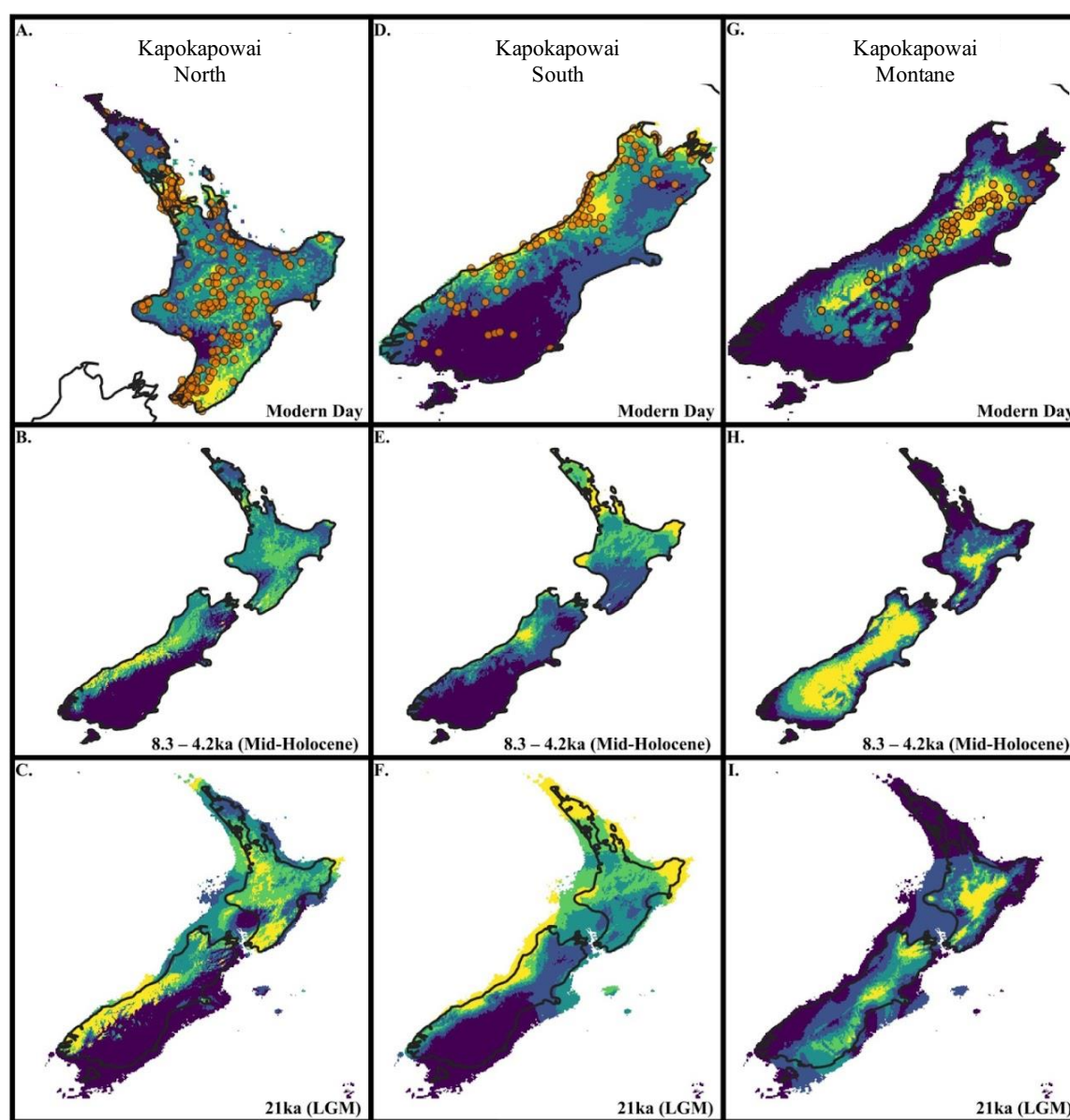


**Kapokapowai
South**

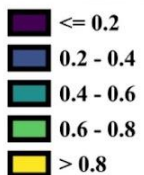


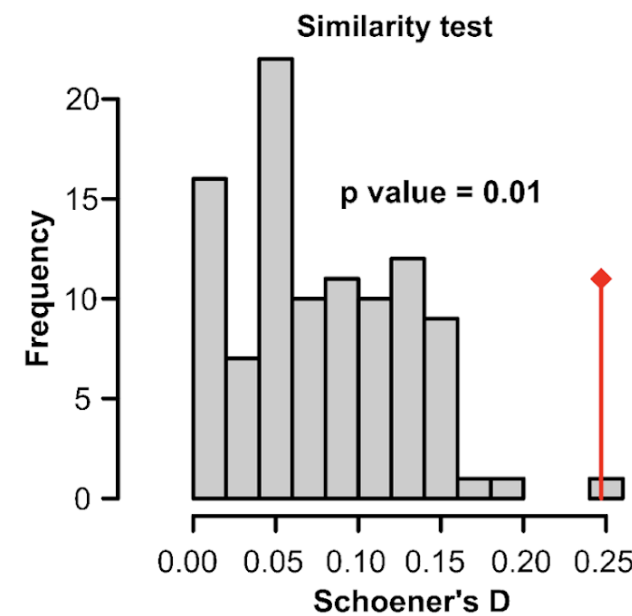
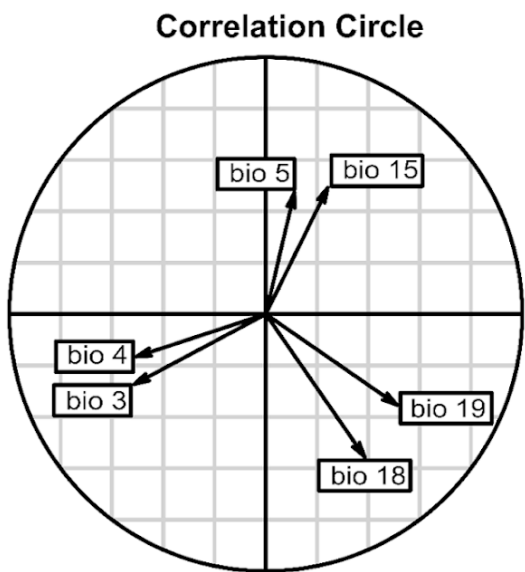
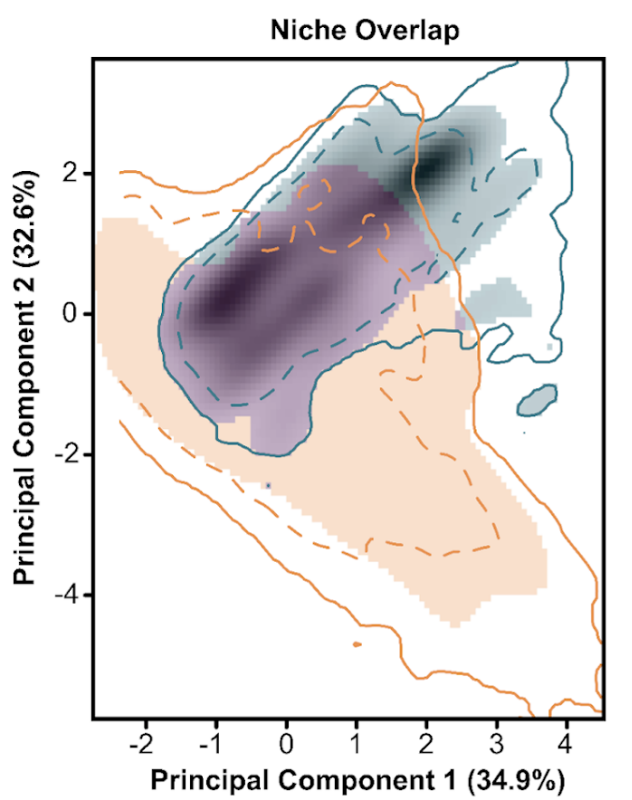
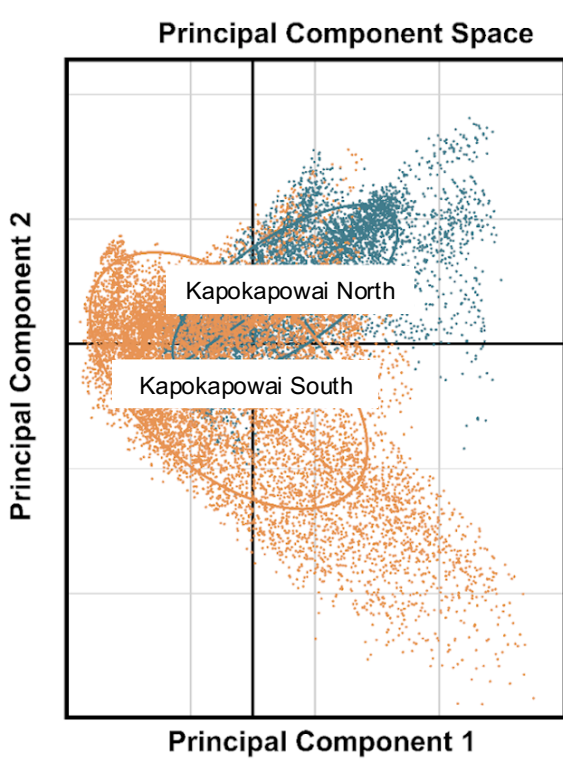
**Kapokapowai
South**

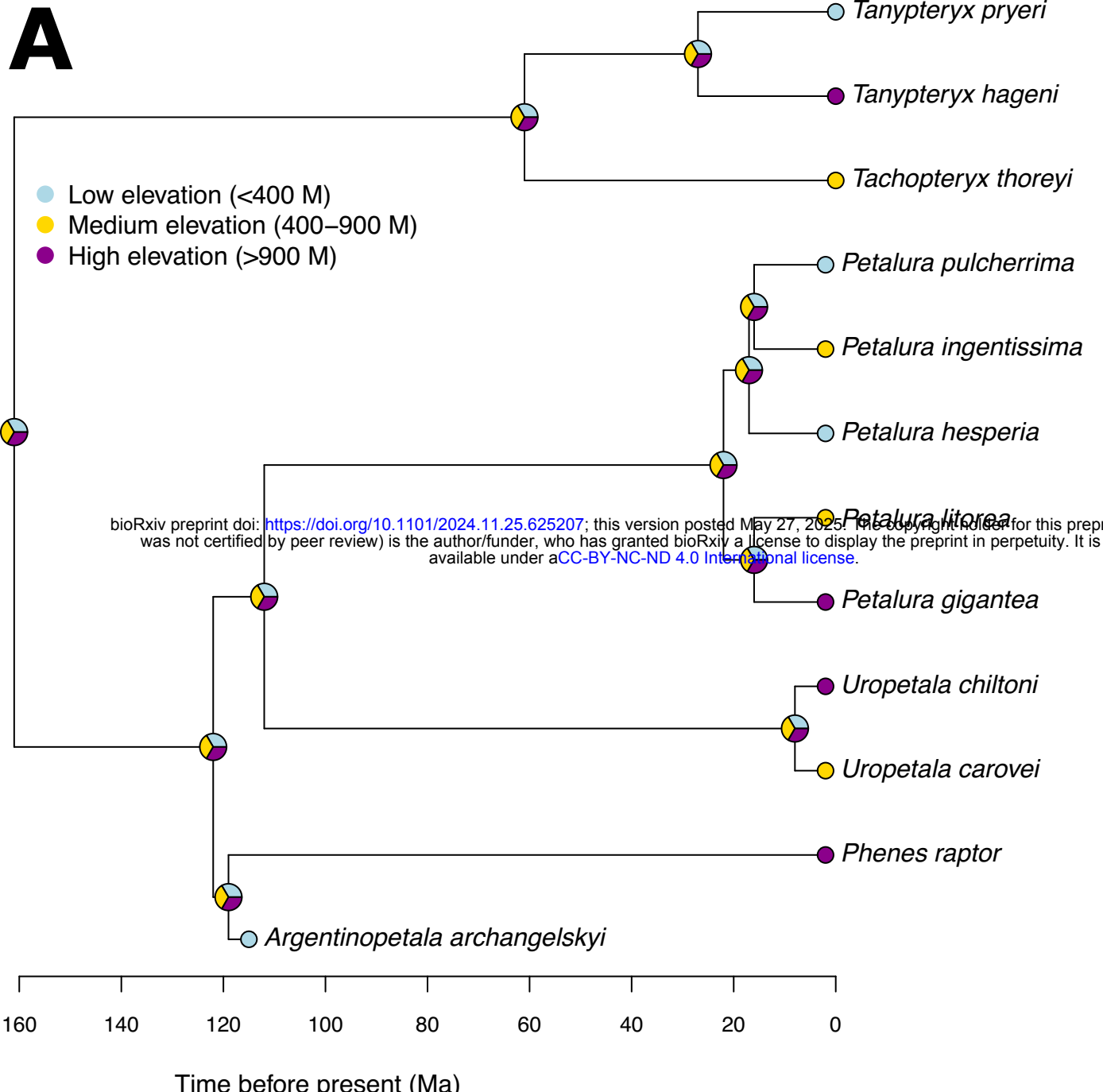
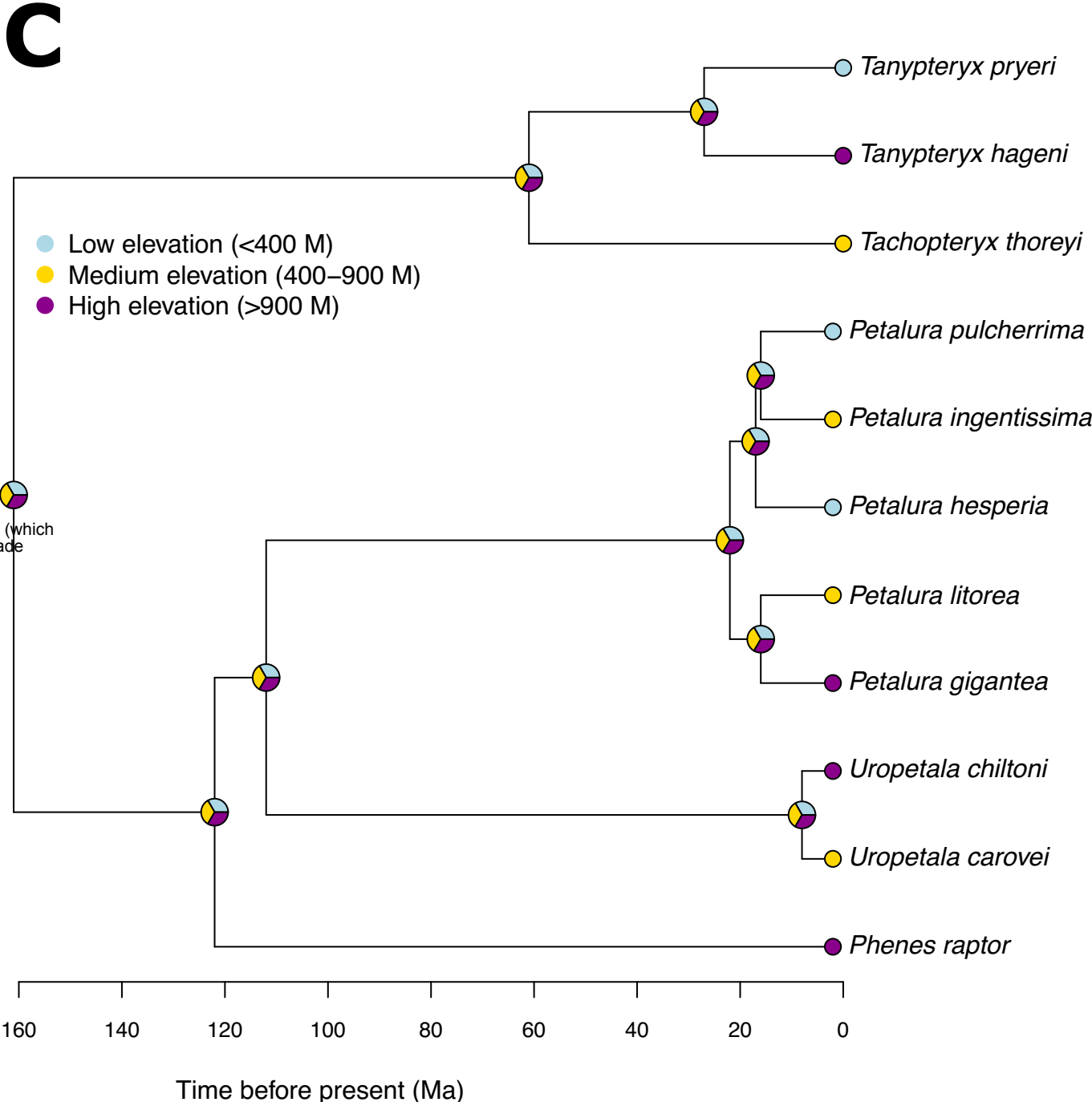
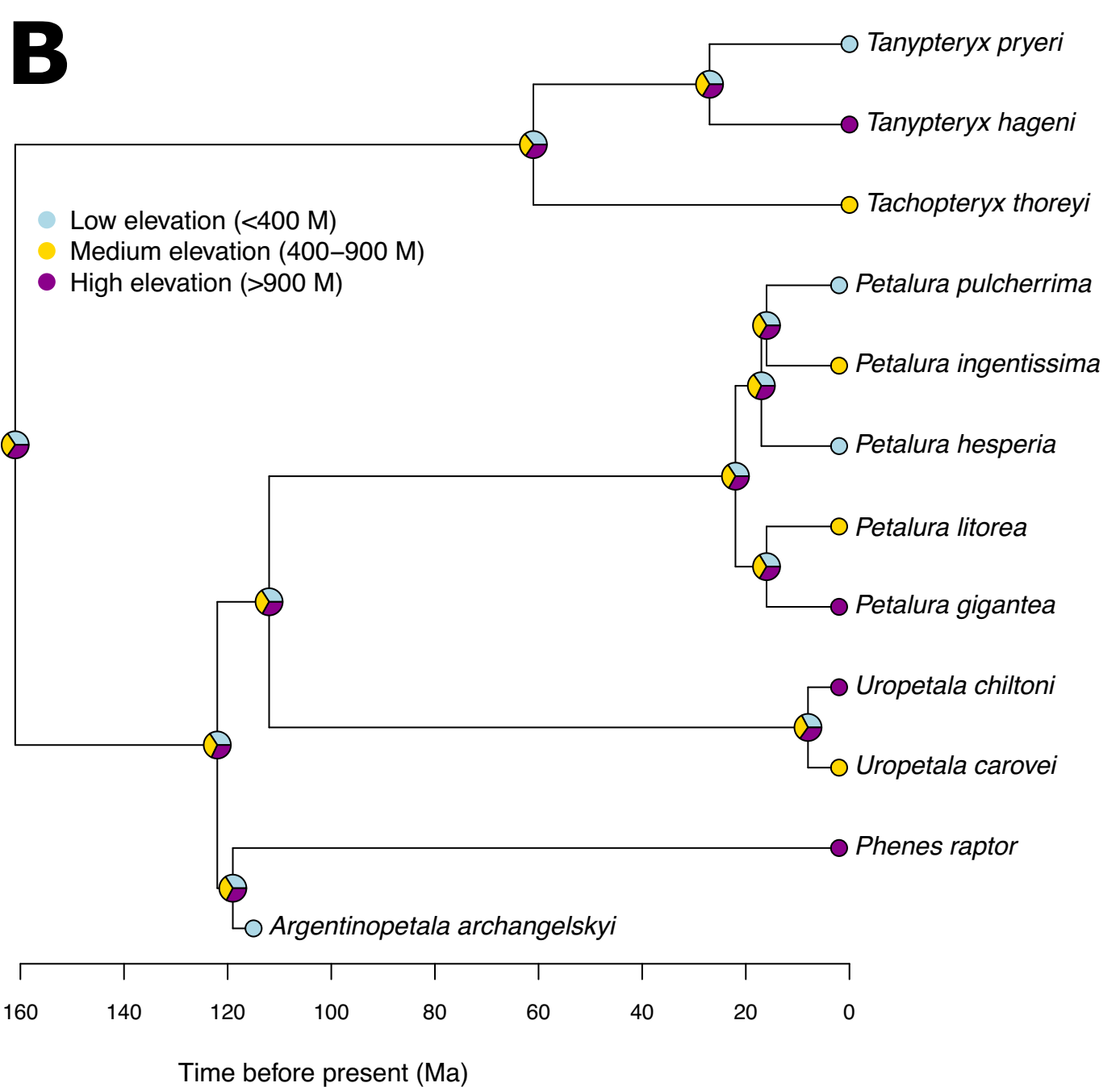
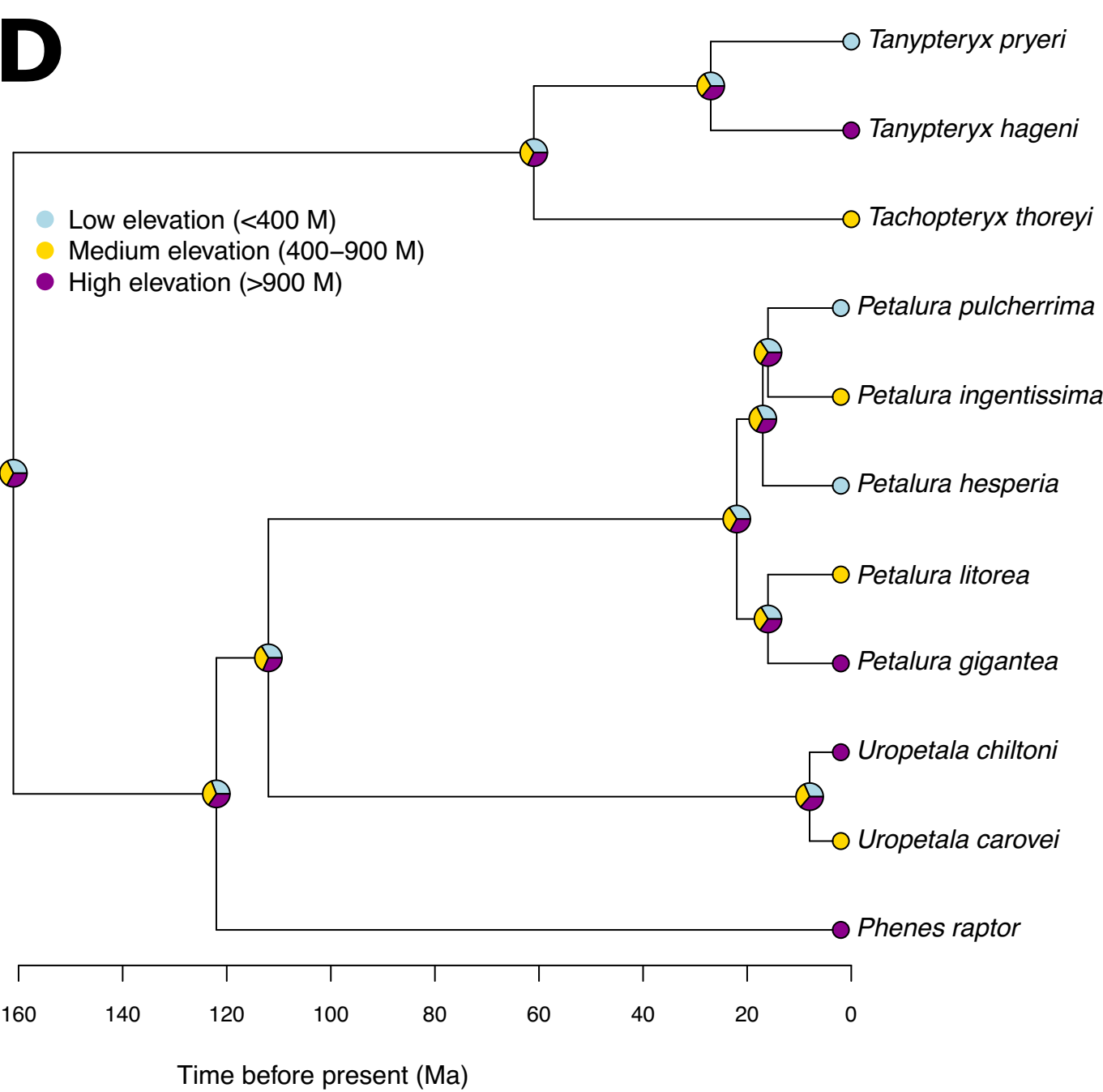




Predicted Suitability





A**C****B****D**

Time before present (Ma)

Time before present (Ma)